

McMaster Nuclear Reactor  
McMaster University  
1280 Main Street West  
Hamilton, Ontario L8S 4K1

(905) 525-9140 Ext 24065  
Fax: (905) 528-4339

MNR Technical Report 97-04

**Thermalhydraulic Modelling  
of the  
McMaster Nuclear Reactor**



Prepared by: \_\_\_\_\_ Date: \_\_\_\_\_  
Wm. J. Garland, Reactor Analyst

Approved by: \_\_\_\_\_ Date: \_\_\_\_\_  
Frank Saunders, Reactor Manager

June 15, 1997

# Table of Contents:

Chapter 1	Introduction .....	1-1
1.1	Preamble .....	1-1
1.2	Document Layout .....	1-2
Chapter 2	MNR Core Assemblies .....	2-1
2.1	Overview .....	2-1
2.2	The MNR 18 Plate Assembly .....	2-1
2.3	The PTR 10 Plate Assembly .....	2-7
2.4	The Shim Assembly .....	2-8
2.5	The Reflector Assembly .....	2-9
2.6	The MNR MAPLE Pin Assembly .....	2-10
Chapter 3	Core Hydraulic Models .....	3-1
3.1	Overview .....	3-1
3.2	Core Main Flow .....	3-1
3.3	Core Bypass Flow .....	3-2
3.4	INVOL and OUTVOL .....	3-3
Chapter 4	System Modelling (CATHENA) .....	4-1
4.1	Overview .....	4-1
4.2	Control Parameters .....	4-2
4.3	Components .....	4-2
4.4	Connections .....	4-6
4.5	Boundary Conditions .....	4-6
4.6	System Models .....	4-6
4.7	System Control .....	4-8
4.8	Initial Conditions .....	4-9
4.9	Heat Transfer Package .....	4-9
Chapter 5	CATHENA Test and Scoping Runs .....	5-1
5.1	Edward's Pipe Blowdown .....	5-1
5.2	MAPLE Pin Test Loop .....	5-2
5.3	MAPLE Single Pin for MNR Conditions .....	5-2
5.4	Single Plate Assembly .....	5-2
5.5	MNR Plate Core Simulation (all 18 plate assemblies) .....	5-3
5.6	HT System Flow Lock-On .....	5-3
5.7	HT System $\Delta T$ Lock-On .....	5-4
5.8	Low Power Thermosyphoning .....	5-4
5.9	MNR Current Plate Core Simulation .....	5-5
Chapter 6	Conclusion .....	6-1
6.1	MNR Plate Assembly Margin .....	6-1
6.2	MNR-MAPLE Pin Assembly Margin .....	6-1
6.3	Code Lock-On .....	6-1

References .....	7-1
Appendix 1 Typical CATHENA Input File Listing .....	8-1

## List of Figures:

<b>Figure 2.1</b> MNR core .....	2-11
<b>Figure 2.2</b> 18 plate assembly top view .....	2-11
<b>Figure 2.3</b> 18 plate assembly schematic .....	2-11
<b>Figure 2.4</b> CATHENA representation of a rectangular channel .....	2-12
<b>Figure 2.5</b> Radius detail for 18 plate fuel .....	2-12
<b>Figure 2.6</b> 10 plate assembly top view .....	2-13
<b>Figure 2.7</b> Radius detail for 10 plate fuel .....	2-13
<b>Figure 2.8</b> Shim Control assembly with 9 fuel plates and a central absorber .....	2-14
<b>Figure 2.9</b> Control absorber inside flow path .....	2-14
<b>Figure 2.10</b> Reflector assembly cross section .....	2-14
<b>Figure 2.11</b> MNR MAPLE fuel pin .....	2-15
<b>Figure 2.12</b> MNR-MAPLE assembly .....	2-15
<b>Figure 3.1</b> Core Configuration (# 48C) as of January 8, 1997 .....	3-5
<b>Figure 3.2</b> Core area of the MNR .....	3-6
<b>Figure 3.3</b> Nodal representation of the core .....	3-6
<b>Figure 3.4</b> Grid plate layout .....	3-7
<b>Figure 3.5</b> Snout hole and bypass hole detail .....	3-7
<b>Figure 3.6</b> Bypass flow geometry in the assembly region .....	3-8
<b>Figure 3.7</b> Bypass flow assignment .....	3-9
<b>Figure 4.1</b> McMaster Nuclear Reactor flowsheet .....	4-10
<b>Figure 4.2</b> CATHENA representation of MNR .....	4-11
<b>Figure 4.3</b> Plenum region .....	4-12
<b>Figure 4.4</b> Elevations in the core area .....	4-13
<b>Figure 4.5</b> Outlet piping layout .....	4-14

## List of Tables:

<b>Table 5.1</b> Flows and temperatures for MNR (base case: core 48c) .....	5-6
---	-----

# Chapter 1 Introduction

## 1.1 Preamble

Thermalhydraulic analysis is required for:

- assessment of the Jan 94 incident
- license renewal
- conversion to LEU pin fuel
- possible operation with more than 8 PTR fuel assemblies
- the possibility of conversion to LEU plate fuel
- in general, for the assessment of any core configuration that lies outside the operating license
- research and operational support.

The use of unqualified computer codes is unacceptable for licensing and safety analysis. It was agreed by all parties that the use of AECL codes was the most expedient route. In the thermalhydraulic area, the initial focus is on CATHENA. The sub-channel code, ASSERT, will be used only if and when necessary. ASSERT is not needed for plate fuel since there are no sub-channels in plate fuel assemblies. ASSERT will only be needed for MAPLE pin type fuel analysis to the extent that the MAPLE specific correlation in CATHENA prove inadequate.

MNR consists of a gravity driven outflow from the large pool through the core to the hold-up tank (HUT). The heat transport system (HTS) pump and associated piping serve only to return this flow to the pool via the heat exchangers (HXs). Consequently, the models for the pump, heat exchangers and associated piping are not the focus of attention herein. Models for safety analysis purposes appropriately centre on the core heat transfer and fluid mechanics. For a small light water moderated core such as MNR, reactor physics coupling via point kinetics is sufficient.

This document details the thermalhydraulic model specification of MNR for the simulation code CATHENA. The thermalhydraulic model was systematically build up in the following order:

- Fuel assembly models (plate and pin types)
- Pool and plenum models
- Outlet section of the HTS including the HUT
- Inlet section of the HTS including the HT pump and HXs
- HUT level control
- Reactor physics (point kinetics) model
- Reactor trip models
- Flapper hydraulics model
- Refinement of the core model.

Testing took place as each addition was made, providing a progressive refinement of the model. This approach proved conducive to model testing and verification. Scoping simulations for typical safety related events (steady state operation at various powers, thermosyphoning, loss of regulation, etc.) provided useful feedback and helped to guide the model refinement process.

## **1.2 Document Layout**

Chapters 2-4 cover the systematic building of the component models, starting with the MNR fuel and reflector assembly models (chapter 2), the core as a collection of assemblies (chapter 3), and the heat transport system (chapter 4). The progressive testing is summarized in chapter 5.

## Chapter 2 MNR Core Assemblies

### 2.1 Overview

The MNR core currently operates at 2000 kW. Typically there are 36 fuel assemblies arranged in a 9×6 square array along with 18 reflector / irradiation sites. One such assembly is depicted in figure 2.1. The core configuration is discussed in detail in chapter 3. Herein, the focus is on the CATHENA models for the plate type fuel assemblies.

The nominal fuel assembly is the 18 plate design. The MNR core also has 8 PTR 10 plate fuel assemblies. The third assembly type is the shim control rod assembly which is essentially an 18 plate assembly with the centre plates removed to allow room for a control rod insertion. A fourth assembly type is the reflector assembly, used both as a reflector and as a holder for irradiation samples. All these existing assembly types are discussed in this chapter. In addition, a proposed fuel assembly based on the MAPLE pin fuel is discussed.

### 2.2 The MNR 18 Plate Assembly

#### 2.2.1 Hydraulics

The 18 plate MNR fuel assembly is composed of 16 fuel plates and 2 outside dummy plates configured as shown in figures 2.2 and 2.3. There are 17 flow cells associated with the 16 active plates.

The flow area for one cell = 0.289 cm × 6.632 cm = 1.91665 cm<sup>2</sup>. Hence, the flow area for 17 cells = 17 × 1.91665 = **32.583 cm<sup>2</sup>**.

The wetted Perimeter = 17 × 2 (6.632 + 0.289) = 235.314 cm. The equivalent diameter is  $De = 4 A / P = 4 \times 32.583 / 235.314 = 0.55386$  cm.

The mass flow at  $v = 1$  m / sec. (nominal) is

$$\begin{aligned} W = \rho v A &= 992 \frac{\text{kg}}{\text{m}^3} \times \frac{1 \text{ m}}{\text{s}} \times 32.583 \times 10^{-4} \text{ m}^2 \\ &= 3.232 \text{ kg/s} \end{aligned}$$

The channel length for the fuel meat is 60 cm.

#### 2.2.2 Heat Transfer Geometry

CATHENA treats the heat transfer in fuel channels as radial heat transfer in pipes. Hence, the rectangular flow cells of MNR Plate assemblies will have to be modelled as equivalent annular flow cells as illustrated in figure 2.4. The 16 plates are paired to form 8 pipes or cells. Each cell has an inner heat transfer surface and an outer heat transfer surface. Since all 8 cells are identical, all surfaces are associated with a single coolant volume.

Each plate is an U-Al section of thickness 0.020" (0.0508 cm) with Al clad of thickness 0.015" (0.0381 cm)

on either side of the fuel meat. We need to preserve the total heat transfer area and solid volume. We treat each plate pair together (8 pairs) making 8 equivalent tubes per assembly. Each tube has an outside radius of  $r_o$ .

The total surface area -  $16 \times 2 \times 6.632 \text{ cm}^2$  per cm of plate length which must equal  $8 \times (2\pi r_o + 2\pi(r_o - 0.127))$ , the surface area of 8 equivalent tubes. Thus:

$$\begin{aligned} r_o &= \frac{16 \times 2 \times 6.632 + 8 \times 2\pi \times 0.127}{8 \times 2\pi \times 2} \\ &= \frac{2 \times 6.632 + \pi \times 0.127}{2\pi} \\ &= 2.1745 \end{aligned}$$

The various radii (see figure 2.5) are thus:

$$\begin{aligned} \text{outside radius of annulus} &= 2.1745 \text{ cm.} \\ \text{outside radius of fuel meat} &= 2.1745 - 0.0381 = 2.1364 \text{ cm.} \\ \text{inside radius of fuel meat} &= 2.1364 - 0.0508 = 2.0856 \text{ cm.} \\ \text{inside radius of annulus} &= 2.0856 - 0.0381 = 2.0475 \text{ cm.} \end{aligned}$$

$$\begin{aligned} \text{Total plate volume/cm length} &= 16 \times 6.632 \times 0.127 \\ &= 13.476 \text{ cm}^3/\text{cm.} \end{aligned}$$

$$\begin{aligned} \text{Total tube volume/cm length} &= 8 \times \pi (r_o^2 - r_i^2) \\ &= 8 \times \pi (2.1745^2 - 2.0475^2) \\ &= 13.476 \text{ cm}^3/\text{cm,} \end{aligned} \quad \text{check ok.}$$

The temperature distribution through the simulated "plate" will be slightly asymmetric since the inside area of the tube is slightly less than the outside area ( $2\pi \times 2.0475$  compared to  $2\pi \times 2.1745$  or a difference of 5.8%). Since Al is a good conductor, the temperature rise in the plate is small, minimizing the effect of this small difference.

$$\text{The heat transfer area / assembly} = 16 \times 2 \times 6.632 \times 60 \text{ cm}^2 = 12,733.4 \text{ cm}^2 = 1.2733 \text{ m}^2.$$

### 2.2.3 Comparison to CANDU

For the purposes of a quick comparison to CANDU, assume a peak assembly power of  $2000 / 35 \times 1.5 = 87.51$  kW.

Assuming a cosine axial power profile, the mid height power / aver =  $\pi / 2$ . Therefore the peak heat flux is

$$q''_{Peak} = \frac{87.51 \times 10^3 \text{ W}}{1.2733 \times 10^4 \text{ cm}^2} \times \frac{\pi}{2} = 10.79 \text{ W/cm}^2$$

and the average core heat flux is

$$q''_{aver} = \frac{57.15 \times 10^3 \text{ W}}{1.2733 \times 10^4 \text{ cm}^2} = 4.49 \text{ W/cm}^2$$

For a 6.5 MW CANDU maximum power channel (12 bundles) we have

$$\frac{6.5 \times 10^6 \text{ W}}{12 \text{ bundles} \times 37 \text{ pins/bundle}} = 1.464 \times 10^4 \text{ W / pin.}$$

Surface area of 1 pin  $\sim 50 \text{ cm} \times \pi (0.65)^2 = 66.36 \text{ cm}^2$ , thus the peak heat flux is

$$\frac{1.464 \times 10^4 \text{ W/pin}}{66.36 \text{ cm}^2/\text{pin}} \times \frac{\pi}{2} = 346 \text{ W/cm}^2$$

Thus

$$\frac{q''_{\text{CANDU}}}{q''_{\text{MNR plate}}} \sim \frac{346}{10.79} \sim 32$$

But, of course, CANDU channel velocity is  $\sim 10 \text{ m/s}$  compared to about  $1 \text{ m/sec}$  for MNR.

#### 2.2.4 Heat Transfer Coefficients

Convective heat transfer is strongly dependent on the hydraulics, notably on velocity and flow regime, as well as on the material properties. MNR operates exclusively in single phase liquid mode under normal operation. The coolant is normally highly subcooled, even near the fuel sheath surface. If coolant flow is impaired sufficiently or if power should rise sufficiently, the coolant - sheath interface temperature will rise to or above the saturation temperature of the coolant ( $117^\circ\text{C}$  in this case). To get a feel for the system response at the onset of significant void, consider the simple coolant energy balance:

$$Q = W (h_{\text{sat liq}} + x h_{\text{fg}} - h_{\text{inlet}})$$

where  $Q$  = assembly power, kW

$W$  = assembly mass flow, kg/s

$x$  = assembly exit quality, fraction

$h_{\text{sat liq}}$  = saturation enthalpy, kJ/kg

$h_{\text{fg}}$  = latent heat of vapourization, kJ/kg

$h_{\text{inlet}}$  = inlet enthalpy, kJ/kg.

If

$$\begin{aligned} Q_{\text{sat}} &= W (h_{\text{sat liq}} - h_{\text{inlet}}) \\ &\approx 3 \text{ kg/s} (490.5 - 125.8) \text{ kJ/kg} \\ &\approx 1100 \text{ kW} \end{aligned}$$

is the power required to bring the coolant up to saturation temperature, then

$$Q_{\text{two phase}} = W (x h_{\text{fg}})$$

is the relationship between the bulk quality and the power associated with boiling. For a high power assembly,  $Q \sim 100 \text{ kW}$ ,  $W \sim 2.3 - 3 \text{ kg/s}$  and  $h_{\text{fg}} \sim 2200 \text{ kJ/kg}$ . Hence, a 1% increase in power beyond that needed to bring the coolant to saturation will generate a quality of  $0.01 \times 100 \text{ kW} / (3 \text{ kg/s} \times 2200 \text{ kJ/kg}) = 0.00015$  weight fraction. This is a very small amount of quality but, from steam tables, the density of steam at 180 kPa is almost 1000 times the liquid volume. The void fraction equivalent of this quality is 0.12, ie 12% by volume of the coolant is vapour. Note also that, from the heat balance above, an overpower of about 10 times (depending on assembly mass flow) will generate bulk boiling. Hence we expect the CPR to be at least 8.5 -

10 based on bulk boiling being an early indicator of a heat transfer crisis.

Vapour generation in the coolant is not a crisis in itself but the onset of significant vapour quality yields large voids (since the system pressure and coolant velocities are low) and possible flow instabilities, vapour blanketing and sheath dryout. The transition from nominal cooling to a heat transfer crisis is sharp and is not easily modelled. Hence, for MNR, it is assumed herein, to be conservative, that the onset of significant boiling represents a safety limit. It follows that it is more meaningful to focus on the determination of the heat transfer coefficient rather than the critical heat flux so as to be able to predict the sheath surface temperature's approach to saturation as accurately as possible during event scenarios. Consequently, herein, we are concerned primarily with single phase liquid flow heat transfer.

For MNR 18 plate assemblies at 2 MW nominal conditions:

- velocity,  $v = 0.83$  m/s
- equivalent hydraulic diameter,  $De = 0.55$  cm
- density,  $\rho = 947$  kg/m<sup>3</sup>
- dynamic viscosity,  $\mu = 238 \times 10^{-6}$  kg/m-s [HAA84]
- heat capacity,  $C_p = 4.2 \times 10^3$  J/kg °C [HAA84]
- heat conductivity,  $k = 0.68$  W/m °C [HAA84]

Hence Reynolds number,  $Re = \rho v De / \mu \approx 18,000$ . According to Incropera [INC90, chapter 8], the onset of turbulence occurs at  $Re$  of about 2,300 with fully turbulent flow by  $Re$  of 10,000. Hence we can safely assume that the nominal core flow is turbulent.

The Prandtl number,  $Pr = \mu C_p / k = 1.47$ .

For turbulent flow it is acceptable to use pipe correlations for channel flow [INC90]. The Dittus Boelter correlation,  $Nu$  (Nusselt number =  $h De / k$ ) =  $0.023 Re^{0.8} Pr^{0.4} = 69$ , where  $h$  is the heat transfer coefficient, is appropriate. For the values of  $De$  and  $k$  above, a  $Nu$  of 69 translates into an  $h$  of approximately 8500 W/°C. The recommended heat transfer correlation (default) in CATHENA is the modified Chen correlation which provides a smoother transition between heat transfer regimes. Typical  $h$  values generated by CATHENA are in the range of 6000 to 8000 W/°C.

For laminar flow, such as might occur under thermosyphoning conditions, pipe correlations are not applicable. However,  $Nu \sim 6.49$  to  $8.23$  for a channel width to thickness ratio of 8 or greater [INC90] (MNR plate assemblies have a width to thickness ratio of 23 for 18 plate fuel and 10 for the 10 plate fuel). Note that for laminar flow,  $Nu$ , and hence  $h$ , is independent of velocity; that is, the heat transfer is solely determined by heat conduction through the boundary layer. CATHENA uses the turbulent correlation (modified Chen in this case) in general but reverts to a limiting  $Nu$  at low flows, consistent with the above observations.

For thermosyphoning, the flow in a channel will be governed by the channel density (ie local power) and the overall channel resistance (again dominated by the exit and entrance losses of the assembly). The resistance through the plenum and flapper hole is negligible. Channel flow instabilities are possible at or near boiling since parallel channels exist and hydraulic resistances are low.

In summary, for forced flow in narrow channels, pipe correlations such as Dittus Boelter can be used. For laminar flow, the Nusselt number is constant, ie heat transfer is independent of velocity. Thus, for forced flow

we know velocity (see Sections 5.6 and 5.9) and we have a reliable heat transfer correlation. For laminar flow the velocity is uncertain but we do not need to know it to get the nominal heat transfer coefficient. Since a fuel sheath surface temperature close to the coolant saturation temperature is a good indication of the approach to dryout, an exact knowledge of CHF is not necessary.

To support the above approach, CHF correlations for plate geometries were investigated. The only correlation supported by CATHENA that is suitable for plate geometries is that of Mirshak [MIR59]. Mishima [MIS87] provides an excellent review of CHF for low velocity and pressure situations, including channel flow. Mishima compares various CHF correlations and shows the Mirshak correlation to be comparable to others in its range of applicability (5 to 45 ft/s, 5-75 C subcooling, 25-85 psia, De 0.21-0.46", vertical downflow, channel geometry - all suitable to MNR plate type assemblies at nominal power conditions except for velocity.

The Mirshak correlation (CATHENA Theoretical Manual, pg A-18) [CAT95] is:

$$q''_{CHF} = 1.51 \times 10^6 [1 + 0.0097 v_m] [1 + 9.14 \times 10^{-3} \Delta T] [1 + 1.896 \times 10^{-1} P]$$

where

$$v_m = \frac{G_{mix}}{\alpha_g \rho_g + [1 - \alpha_g] \rho_f} \quad m/s$$

$$P = \text{total pressure} \times 10^{-5} \quad \text{Bar}$$

$$\Delta T = \max[0, T_f^{sat} - T_f] \quad ^\circ C$$

For MNR 18 plate assemblies:

$$v_m \approx 0.83 \quad m/s$$

$$P \approx 1.8 \quad \text{Bar}$$

$$\Delta T \approx 0 \quad ^\circ C$$

giving a CHF of  $\sim 2.2 \times 10^6 \text{ J/m}^2\text{s}$ . The nominal heat flux is  $\sim 0.1 \times 10^6 \text{ J/m}^2\text{s}$  giving a CPR of  $\sim 22$ . This is agreement with CATHENA output. Note that velocity, and hence  $v_m$  will vary from case to case but the correlation is not particularly sensitive to variations in  $v_m$  ( a 10% variation in  $v_m$  gives  $\sim$  a 1% variation in CHF. To assess the applicability of the Mirshak correlation at velocities lower than 5 ft/s (1.5 m/s), we turn to Mishima's comparison of the Mirshak correlation to other correlations. Mishima defines a dimensionless volumetric mass flow

$$G^* \equiv \frac{G}{\sqrt{\lambda \rho_g g \Delta \rho}}$$

and a dimensionless heat flux

$$q^* \equiv \frac{q}{h_{fg} \sqrt{\lambda \rho_g g \Delta \rho}}$$

where

$$\lambda = \sqrt{\frac{\sigma}{g \Delta \rho}} \quad \text{and } \sigma = \text{surface tension}$$

The MNR values are

$$\lambda = \sqrt{\frac{0.055}{9.81 \times 946}} = 0.00243 \text{ m}$$

$$G^* \equiv \frac{947 \times 0.83}{\sqrt{0.00243 \times 0.948 \times 9.81 \times 947}} = 947 \times 0.83 \times 4.63 = 170$$

$$q_{CHF}^* \equiv \frac{2.23 \times 10^6}{2225 \times 10^3 \sqrt{0.00243 \times 0.948 \times 9.81 \times 947}} = 0.216$$

These values correspond to the extreme lower limit of Mirshak's correlation as plotted by Mishima in his figure 8 ( $q^*$  vs  $G^*$ ). Judging by the other correlations evaluated on the same plot, we would expect the Mirshak correlation to yield CHF values that are too high for velocities below 1.5 m/s. This is consistent with the premise that a heat transfer crisis occurs soon after the onset of significant void and that bulk outlet boiling starts at roughly 10 times nominal power, based on the simple heat balance presented at the beginning of this section. Mishima shows that dryout occurs at  $\sim 0$  exit quality under these conditions, confirming the assertion made herein that at low pressure and flow, if significant boiling occurs, a heat transfer crisis is not far off. In effect, exact knowledge of CHF is not required for MNR and, hence, the high predictions of the Mirshak correlation at low velocities is inconsequential. It is sufficient to have a HTC that is sufficiently accurate to determine the sheath surface temperature. If the sheath surface temperature approaches  $\sim 117$  C, then it can be conservatively assumed that a heat transfer limit has been reached. Indeed, significant boiling can lead to flow instabilities for MNR type conditions [MIS87]. CATHENA simulations typically break down under these conditions because of the large volumetric expansion of the vapour phase and the low hydraulic resistances in the parallel paths of the core.

### 2.2.5 Material Properties

U-Al material properties				
Source	Conductivity, k		Volumetric heat capacity, g	
	BTU / hr-ft-°F	J / s-m-°C	BTU / ft³-°F	J / m³-°C
Michigan SAR, p26 [MIC77]	103	(=178.27) Value used in CATHENA		
PARET manual for SPERT test, p98 [OBE69]	$6.39 \times 10^{-7} T^2 + 3.56 \times 10^{-3} T + 12.015$		$-2.159 \times 10^{-6} T^2 + 1.256 \times 10^{-2} T + 55.0$	(= 3.688 x 10 <sup>6</sup> ) Value used in CATHENA
Conversion	1 BTU / hr-ft-°F = 1.7307 J / s-m-°C		1 BTU / ft³-°F = 67.066 x 10 <sup>3</sup> J / m³-°C	

## 2.3 The PTR 10 Plate Assembly

### 2.3.1 Hydraulics

The 10 plate PTR fuel assembly is composed of 10 fuel plates configured as shown in figure 2.6. The outside plates contain fuel, in contrast to the 18 plate design. There are 9 internal flow cells associated with the 10 plates. The plate thickness is 0.060" and the groove-to-groove spacing is 0.319", leaving a coolant passage thickness of 0.259" (0.6579 cm).

The flow area for one cell = 0.6579 cm × 6.632 cm = 4.3632 cm<sup>2</sup>. Hence, the flow area for 9 cells = **39.269 cm<sup>2</sup>**.

The wetted Perimeter = 9 × 2 (6.632 + 0.6579) = 131.22 cm. The equivalent diameter is  $De = 4 A / P = 1.9170$  cm.

The mass flow at  $v = 1$  m / sec. (nominal) is

$$\begin{aligned} W = \rho v A &= 992 \frac{kg}{m^3} \times \frac{1 m}{s} \times 39.269 \times 10^{-4} m^2 \\ &= 3.895 \text{ kg/s} \end{aligned}$$

The channel length for the fuel meat is 60 cm.

### 2.3.2 Heat Transfer

The heat transfer treatment is the similar to that of the 18 plate assembly, i.e., the rectangular flow cells of PTR plate assemblies will have to be modelled as equivalent annular flow cells as illustrated in figure 2.4.

Each plate is an U-Al section of thickness 0.020" (0.0508 cm) with Al clad of thickness 0.020" (0.0508 cm) on either side of the fuel meat. We need to preserve the total heat transfer area and solid volume. We treat each plate pair together (5 pairs) making 5 equivalent tubes per assembly. Each tube has an outside radius of  $r_o$ .

The total surface area - 10 × 2 × 6.632 cm<sup>2</sup>/cm of plate length which must equal 5 × (2π $r_o$  + 2π( $r_o$  - 0.1524)), the surface area of 5 equivalent tubes. Thus:

$$\begin{aligned} r_o &= \frac{10 \times 2 \times 6.632 + 5 \times 2\pi \times 0.1524}{5 \times 2\pi \times 2} \\ &= \frac{2 \times 6.632 + \pi \times 0.1524}{2\pi} \\ &= 2.1872 \end{aligned}$$

The various radii (see figure 2.7) are thus:

outside radius of annulus = 2.1872 cm.

outside radius of fuel meat = 2.1872 - 0.0508 = 2.1364 cm.

inside radius of fuel meat =  $2.1364 - 0.0508 = 2.0856$  cm.  
 inside radius of annulus =  $2.0856 - 0.0508 = 2.0348$  cm.

The temperature distribution through the simulated “plate” will be slightly asymmetric since the inside area of the tube is slightly less than the outside area ( $2\pi \times 2.0348$  compared to  $2\pi \times 2.1872$  or a difference of 7.0%). Since Al is a good conductor, the temperature rise in the plate is small, minimizing the effect of this small difference.

The heat transfer area / assembly =  $10 \times 2 \times 6.632 \times 60 \text{ cm}^2 = 7,958.4 \text{ cm}^2 = 0.7958 \text{ m}^2$ .

### 2.3.3 Material Properties

The materials used in the PTR assemblies are the same as in the 18 plate design.

## 2.4 The Shim Assembly

### 2.4.1 Hydraulics of the fuelled regions

The shim assembly is basically an 18 plate assembly with the central 9 plates removed and a central box added to accommodate control rods. The outer plates contain fuel, in contrast to the 18 plate assembly. The configuration is shown in figure 2.8. There are 9 internal flow cells associated with the 9 active plates.

The flow area for one cell =  $0.289 \text{ cm} \times 6.632 \text{ cm} = 1.91665 \text{ cm}^2$ . Hence, the flow area for 9 cells = **17.250 cm<sup>2</sup>**.

The wetted Perimeter =  $9 \times 2 (6.632 + 0.289) = 124.578 \text{ cm}$ . The equivalent diameter is  $De = 4 A / P = 0.55386 \text{ cm}$ .

The mass flow at  $v = 1 \text{ m / sec}$ . (nominal) is

$$\begin{aligned} W = \rho v A &= 992 \frac{\text{kg}}{\text{m}^3} \times \frac{1 \text{ m}}{\text{s}} \times 17.25 \times 10^{-4} \text{ m}^2 \\ &= 1.711 \text{ kg/s} \end{aligned}$$

The channel length for the fuel meat is 60 cm.

### 2.4.2 Hydraulics of the Control Absorber Region

There are two flow paths through the central control absorber. Figure 2.9 illustrates the flow path through a small opening into the hollow control absorber. The small opening in the control rod has an area of  $0.65'' \times 0.5'' = 2.097 \text{ cm}^2$ . The second flow path is through the narrow gap between the control absorber and the control box walls. Referring to figure 2.8, the gap thickness is  $\frac{1}{2} \times (28.58 \text{ mm} - 24.38 \text{ mm}) = 2.1 \text{ mm}$ . The slot length is 32 mm for a total flow area of  $0.672 \text{ cm}^2$  for two slots. These flow paths are modelled as an orifice of area  $2.097 + 0.672 = 2.769 \text{ cm}^2$  in a pipe of equivalent diameter to the inner cavity of the control rod ( $De = 2.633$

cm, area = 8.431 cm<sup>2</sup>). The outside slots are 33 cm in length and, hence, offers considerably more flow resistance than that of an orifice. Thus, the model will predict a larger bypass flow through the control absorber region than is the actual case. Since this bypass flow takes flow away from the flow past the heated fuel plates, the model is conservative.

#### 2.4.3 Heat Transfer

The heat transfer model is the same as for the 18 plate assembly except that there are now 4.5 pairs of plates per assembly or 27 pairs of plates in total for the 6 shim assemblies. The radii are the same as for the 18 plate assembly model.

The heat transfer area / assembly =  $9 \times 2 \times 6.632 \times 60 \text{ cm}^2 = 7,162.6 \text{ cm}^2 = 0.7162 \text{ m}^2$ .

#### 2.4.4 Material Properties

The materials used in the shim assemblies are the same as in the 18 plate design.

### 2.5 The Reflector Assembly

A cross section of a reflector assembly is shown in figure 2.10. The dominant flow resistance is the 3/4" diameter orifice; the rest of the flow path is at least 1 3/8" in diameter. Hence the flow path is modelled as 60 cm of 1.375" diameter ( $D_e = 3.493 \text{ cm}$ , area = 9.58 cm<sup>2</sup>) pipe containing a 3/4" diameter (2.85 cm<sup>2</sup>) orifice.

## 2.6 The MNR MAPLE Pin Assembly

### 2.6.1 Hydraulics

The MAPLE fuel pin is U-Al meat with an Al clad as illustrated in figure 2.11. It is proposed that the MNR plate fuel be replaced with a 5×5 square array of MAPLE fuel pins as illustrated in figure 2.12. The central pin will be a space dummy pin. The cross sectional area of 1 pin is

$$\begin{aligned} \text{Area/pin} &= \frac{\pi}{4} (7.87)^2 + 8 \times 0.76 \times 1.02 \text{ mm}^2 \\ &= 48.65 \text{ mm}^2 + 6.20 \text{ mm}^2 \\ &= 54.84 \text{ mm}^2 \end{aligned}$$

The flow area for a MNR MAPLE pin assembly is just the total internal cross section area less the cross sectional area of 25 pins. Thus:

$$\begin{aligned} \text{Flow area} &= 7.666 \times 6.632 \text{ cm}^2 - 25 \times 0.5485 \text{ cm}^2 \\ &= 50.84 - 13.71 \text{ cm}^2 \\ &= 37.128 \text{ cm}^2 \end{aligned}$$

This is similar to the flow area of the plate assembly (34.5 cm<sup>2</sup>). Hence the core flow should not be adversely affected by the switch to MAPLE type fuel.

### 2.6.2 Heat Transfer Geometry

The heated length of the assembly is 60 cm. The perimeter =  $\pi D + 16 \times \text{fin height} = 41.04 \text{ mm}$ . Therefore the heat transfer area =  $4.104 \times 60 = 242.26 \text{ cm}^2/\text{pin}$ . For a 24 pin assembly the heat transfer area = 0.591 m<sup>2</sup>/assembly. This is 46.4% of the 18 plate assembly.

The average pin power =  $2000 / (35 \times 24) = 2.38 \text{ kW/pin}$ . The average heat flux is

$$q'' = \frac{2.38 \text{ kW} \times 24}{0.591 \text{ m}^2} = 96.7 \frac{\text{kW}}{\text{m}^2} = 9.67 \text{ W/cm}^2$$

This is 215% of the 18 plate assembly case.

### 2.6.3 Heat Transfer Coefficients and Material Properties

MAPLE pin fuel material properties and correlations for the heat transfer coefficient and for CHF have been developed at AECL and incorporated into CATHENA. The range of applicability includes the MNR conditions.

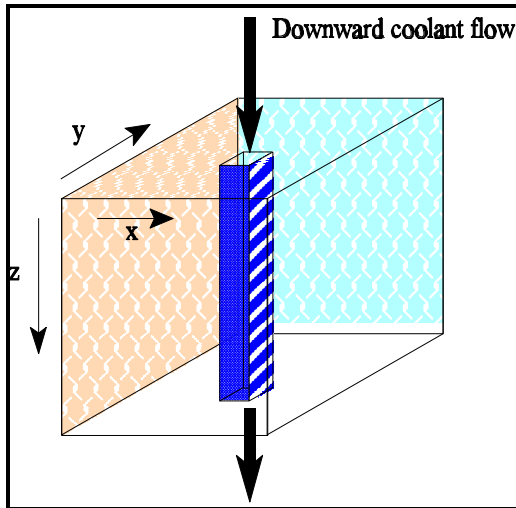


Figure 2.1 MNR core

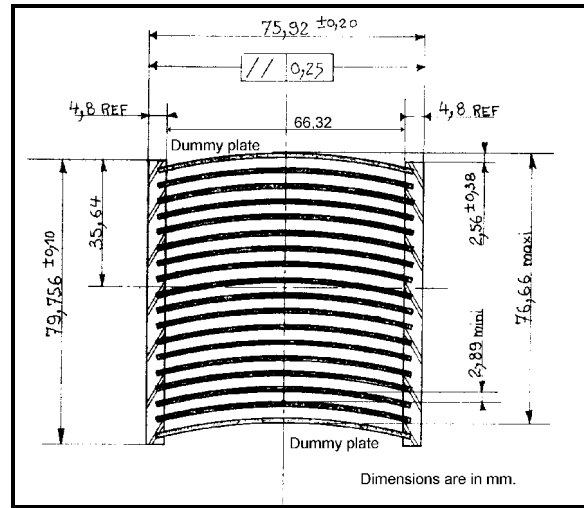


Figure 2.2 18 plate assembly top view

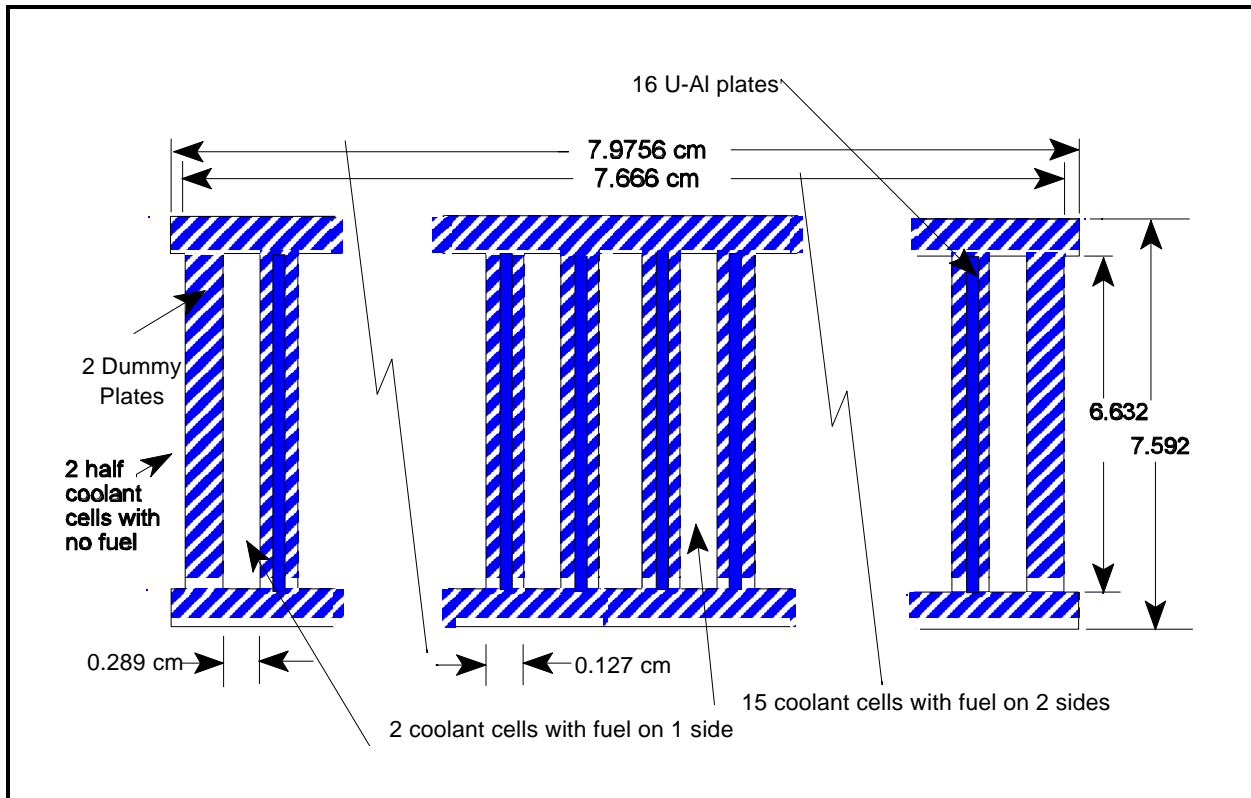


Figure 2.3 18 plate assembly schematic

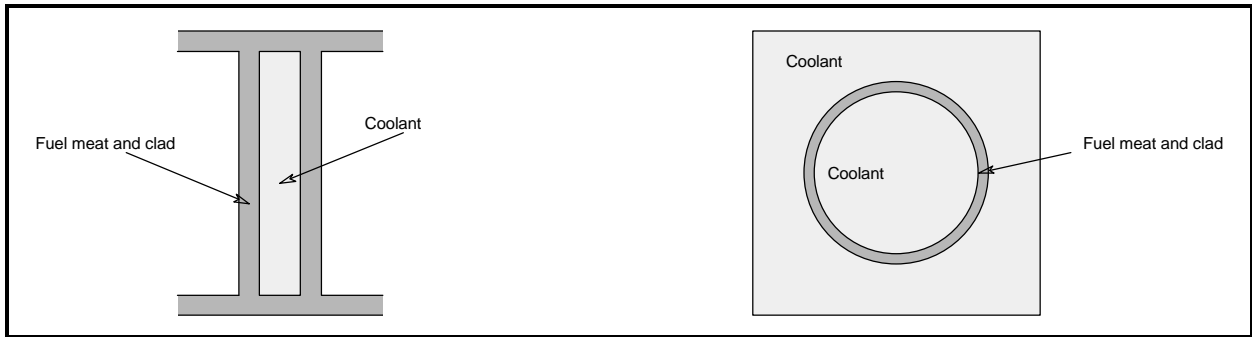


Figure 2.4 CATHENA representation of a rectangular channel

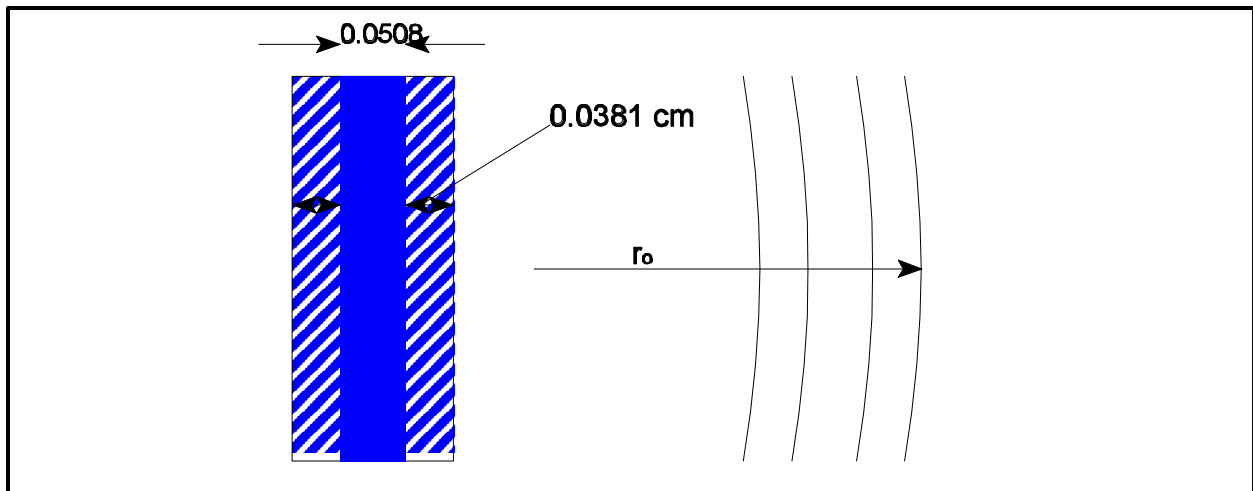


Figure 2.5 Radius detail for 18 plate fuel

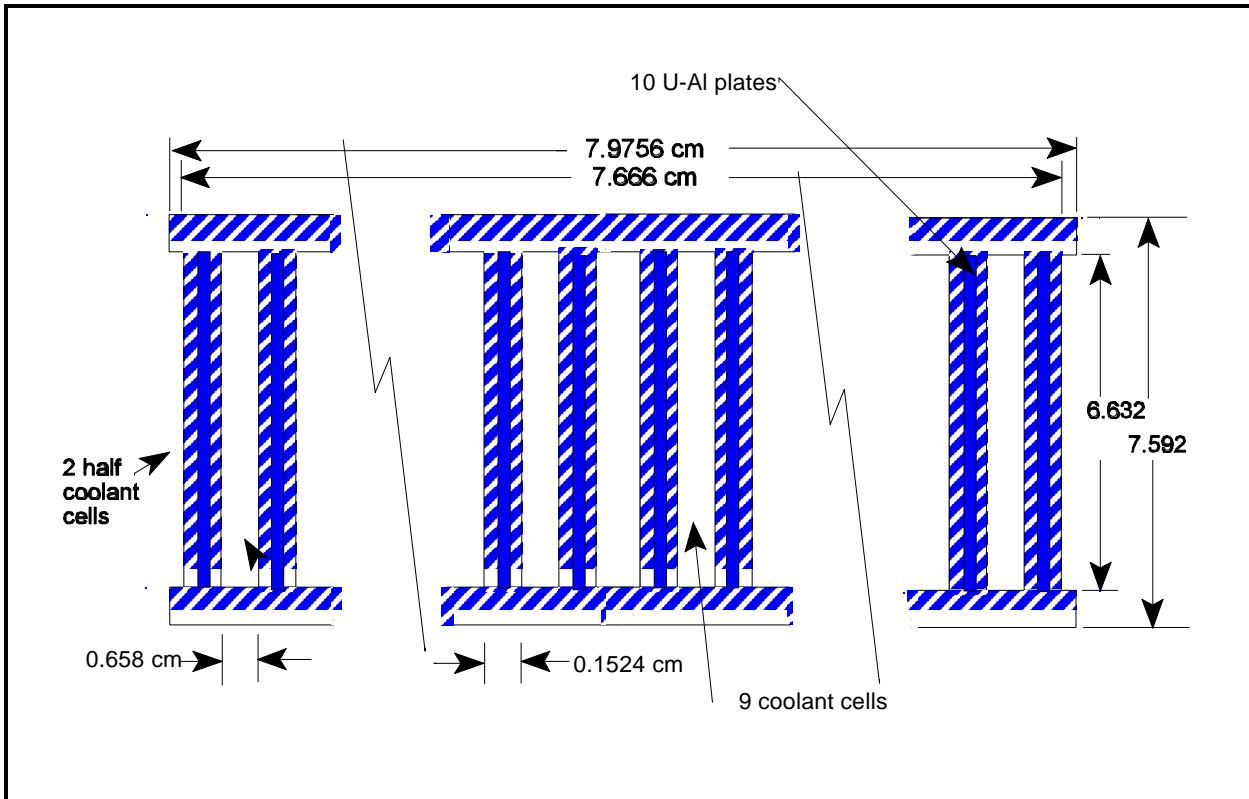


Figure 2.6 10 plate assembly top view

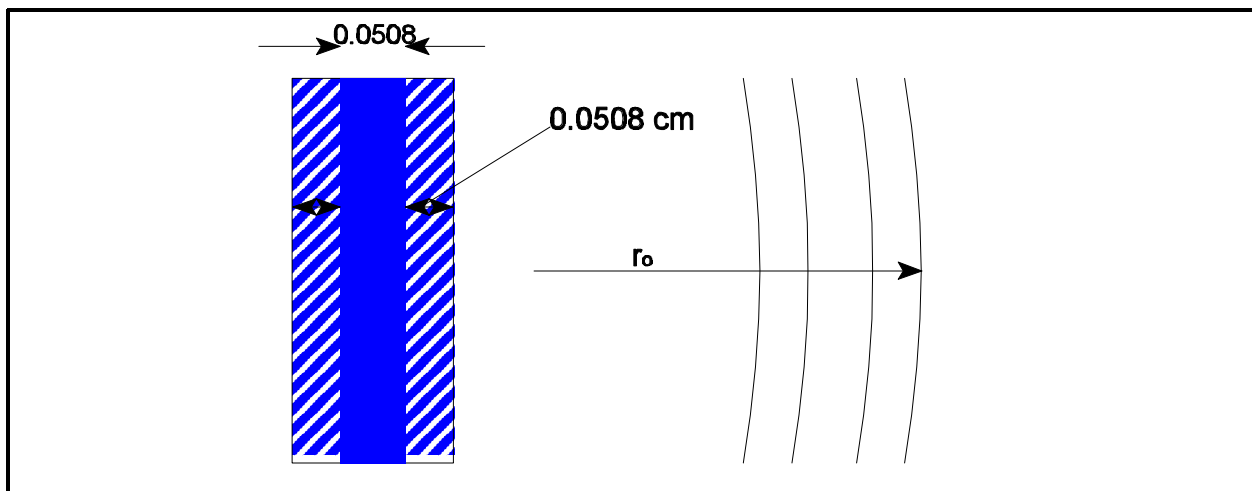


Figure 2.7 Radius detail for 10 plate fuel

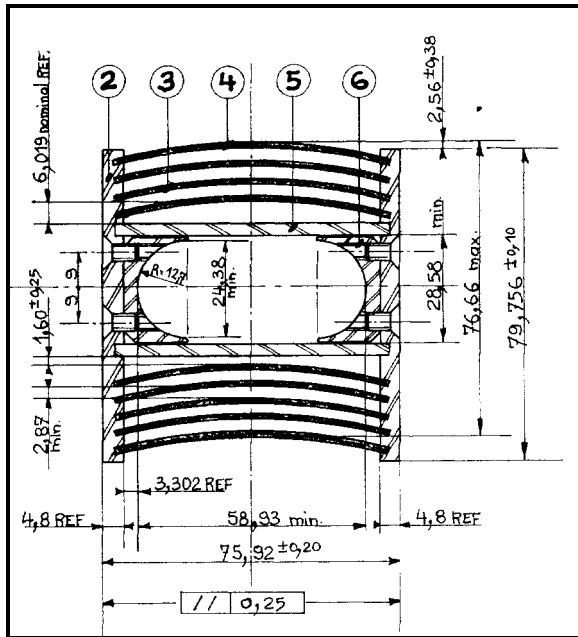


Figure 2.8 Shim Control assembly with 9 fuel plates and a central absorber

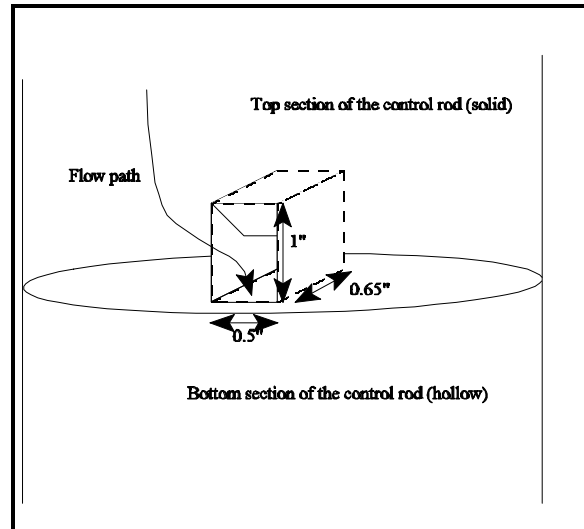


Figure 2.9 Control absorber inside flow path

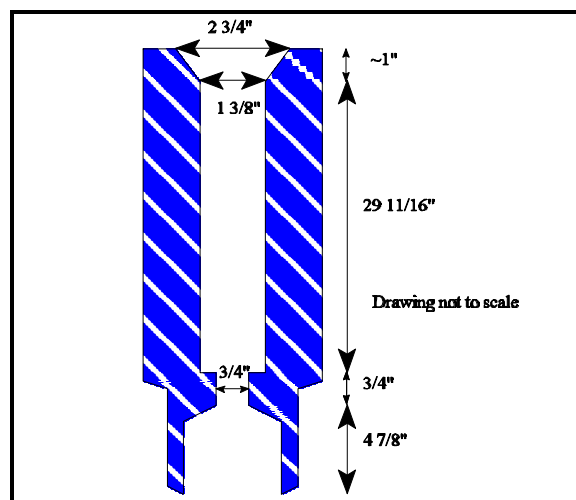


Figure 2.10 Reflector assembly cross section

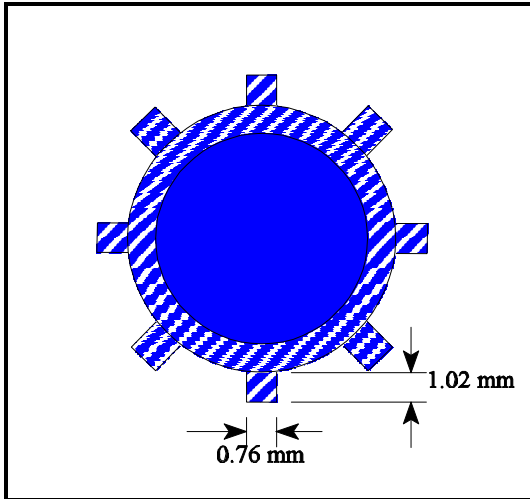


Figure 2.11 MNR MAPLE fuel pin

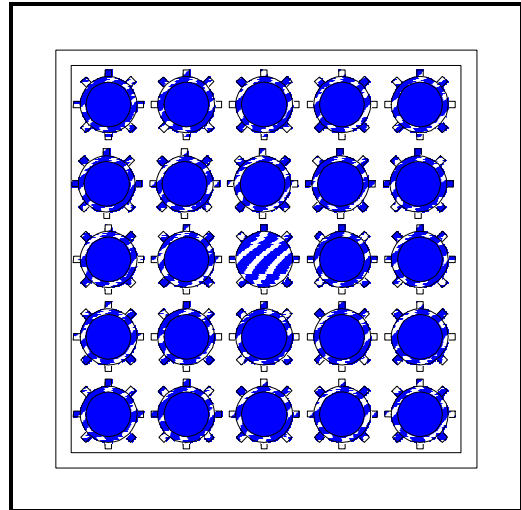


Figure 2.12 MNR-MAPLE assembly

## Chapter 3 Core Hydraulic Models

### 3.1 Overview

The reactor core consists of a  $9 \times 6$  rectangular array of fuel, control, reflector and irradiation assemblies. Figures 3.1 and 3.2 shows the layout of the various types of assemblies. The details of the fuel assembly heat transfer models and hydraulic models are given in chapter 2. This chapter discusses the flow details in and around the core. Chapter 4 discusses the flow in the HTS piping.

### 3.2 Core Main Flow

The bulk of the coolant flow is between the fuel plates and out the snout hole in the grid plate. However, there is an additional flow past the outside of the fuel assemblies and out through small bypass holes in the grid plate. Herein the hydraulic models for the core as a system are discussed. Since the various types of assemblies have different powers, flow cross-sectional areas and heat transfer areas, each group will need to be modelled separately. For the initial stages of CATHENA input development, the core was modelled as 34 average assemblies and 1 high power assembly. Subsequently, the core model was improved to reflect the current core configuration. The groupings for core as of January 8, 1997 (designated 48C) are as follows (see figure 3.3):

MNR18: There are 22 assemblies of the 18 plate design as indicated in figure 3.1. The highest power assembly is modelled separately, leaving 21 assemblies, modelled as parallel assemblies with a total power of 1175 kW.

MNR18HOT: The highest power 18 plate assembly is 4C (123 kW).

APTR: There are 8 assemblies of the 10 plate design (PTR) as indicated in figure 3.1. The highest power assembly is modelled separately, leaving 7 assemblies, modelled as parallel assemblies with a total power of 389 kW.

HPTR: The highest power 10 plate assembly is 4D (113 kW).

HPTROUT: The outside plates of the 10 plate assemblies are partially cooled by bypass flow (discussed below). Since these outer plates might have a substantially different temperature than the inner plates, they are modelled separately.

SHIM: There are 6 control rod assemblies: 5 shim rods and one regulating rod. These assemblies have lower power because of the absorbers and because the assemblies contain 9 fuel plates instead of the normal 16. Specific heat fluxes are lower than the fully fuelled power assemblies; hence a hot assembly is not modelled.

SAMPLES: There are 10 sites containing reflector material with central holes to allow the insertion of irradiation samples. The central hole permits flow through its associated snout hole. The flow is restricted by a 3/4" orifice.

SHIMABS: There is a flow path through the centre of each control rod out the associated snout hole. The flow is restricted.

### 3.3 Core Bypass Flow

Each grid location, except for row 1 and column F, has a 3/4" diameter hole (called a bypass hole) drilled through the grid plate to the north-east of the snout hole (40 bypass holes in all), see figures 3.4 and 3.5. This bypass hole can be plugged but is normally open to provide a bypass flow to provide additional coolant flow to the outside surface of the core assemblies. Currently, there are 35 open bypass holes, the 5 holes between rows 8 and 9 are closed. The shim control assemblies and the 10 plate PTR assemblies have fuel in the outer plates, the 18 plate assemblies do not. The highest power fuel assemblies are modelled separately. Each of these cases present a different cooling configuration with respect to the treatment of the bypass flow, as discussed below.

APTRBYP: The 10 plate assemblies have fuel in all 10 plates. The outer plates are cooled on the inside by the main flow through the snout hole. Cooling to the outside surface of the outer plates is provided by the bypass flow modelled here by the component APTRBYP for the typical (i.e., not high power) assemblies.

HPTRBYP: Since the average 10 plate assembly has a substantially different heat load than the highest power 10 plate assembly, the associated bypass flows are treated separately. The outer plates of the hottest 10 plate assembly is linked to the hydraulic component HPTRBYP.

SHIMBYP: The shim assemblies have fuel in the outer plates like the 10 plate assemblies. Cooling to the outside surface of the outer plates is provided by the bypass flow modelled here by the component SHIMBYP.

COREBYP: The 18 plate assemblies contain 16 active fuel plates and 2 outer dummy plates; hence additional cooling is superfluous. The unheated bypass flow associated with the 18 plate assemblies and reflector sites are modelled by COREBYP.

Figure 3.6 illustrates four 18 plate assemblies and the associated bypass flows. The bypass geometry is the same for the other assembly types. The major flow path lies at the north-south interface of the assemblies, i.e., between rows 1&2, 2&3, 3&4, 4&5, 5&6, 6&7 and 7&8. (Henceforth, the intersections will be identified as I-1/2, I-2/3, etc). Thus an assembly shares its associated bypass flow at its north face with the south face of its northern neighbour. There is negligible sharing in the east-west direction. The bypass holes located beneath the bypass areas collect the bypass flow. An accounting must be done to determine the number of bypasses that are associated with each of the four bypass situations discussed above (APTRBYP, HPTRBYP, SHIMBYP, COREBYP). Flow is assigned to a heated surface by default if that heated surface borders on an unheated surface. Referring to figure 3.7, the table to the right of the core map shows that at I-7/8, for instance, the 10 plate assemblies have the equivalent number of 2 bypass paths that are associated with its heated outer plates. An equivalent of 3 bypass paths are associated with unheated surfaces. The assignment is not critical for the lower power assemblies and the hot 18 plate assembly (since the outer surfaces of 18 plate assemblies are not fuelled) but care should be taken with the 10 plate hot assembly. For this core

configuration, it has 1 equivalent path for I-3/4 and 1 for I-4/5. The totals on the bottom line of the table show the total number of bypass paths associated with each bypass group. These numbers are entered as the last entry in the COMPONENT model for the bypasses in CATHENA, indicating the number of parallel paths associated with that COMPONENT. When modelling different core configurations, this accounting exercise must be repeated.

The bypass hydraulic dimensions and resistances are dependent on the fuel outside dimensions and the grid spacings. From [ERN72]:

$$\text{Flow cross sectional area} = A = 0.179" \times 3.035" + 0.046" (3.189 - 0.179)" = 0.681 \text{ in}^2 = 4.3935 \text{ cm}^2$$

$$\text{Wetted perimeter} = P = 2 (3.035 + 3.189) = 12.44"$$

$$De = 4A/P = 0.2289" = 0.5562 \text{ cm.}$$

$$\text{Length} = 60 \text{ cm.}$$

Although this is in series with the 5" long 3/4" hole through the grid plate, no attempt was made to model the grid hole resistance. The actual flow resistances of this flow configuration are uncertain. This is an area of uncertainty that will directly affect the cooling of fuel assemblies that have fuel in their outer plates.

### 3.4 INVOL and OUTVOL

Each assembly (approximately 7.9 cm × 7.6 cm × 70 cm) has a circular snout at the bottom which is inserted into the grid plate. Below the grid plate is a plenum leading to the outlet piping (as discussed in chapter 4). Coolant flow is downward from the pool (see figure 3.2).

The groupings of assemblies (8 ten plate, 22 eighteen plate, 6 control) represent a range of inlet cross-sectional areas. To prevent CATHENA from applying a different entrance and exit loss to each grouping, a VOLUME component is applied before and after the core parallel paths as shown in figure 3.3.

The active length of the assemblies (from a heat transfer perspective) is 60 cm. Water volume areas above and below the active fuel areas are modelled as part of the connecting VOLUME components. Since the core is modelled as 12 axial nodes, the inlet volume (INVOL) was taken as 1/12 of the core volume since large mismatches in COMPONENT volumes are to be avoided if possible for numerical simulation reasons. The outlet volume (OUTVOL) is the combined volume of the 46 large snout holes (36 fuelled sites plus 10 reflector sites) and the 35 small bypass holes in the grid plate that are open:

$$\text{Volume of each 2" diameter, 5" high snout hole} = 20.628 \text{ cm}^3.$$

$$\text{Volume of each 3/4" diameter, 5" high bypass hole} = 2.850 \text{ cm}^3.$$

$$\text{OUTVOL volume} = 46 \times 20.628 + 35 \times 2.850 \text{ cm}^3 = 0.013318 \text{ m}^3.$$

TANK components cannot be directly connected to VOLUME components. Hence a short PIPE component (INPIPE) was used.

NORTH						
	A	B	C	D	E	F
1	H <sub>2</sub> O	H <sub>2</sub> O	PTR (10) 47 kW	CI (18) 57 kW	CI (18) 32 kW	MNR (18) 17 kW
2	Refl.	MNR (18) 27 kW	SHIM (9) 30 kW	PTR (10) 72 kW	SHIM (9) 33 kW	PTR (10) 51 kW
3	PTR (10) 56 kW	MNR (18) 58 kW	CI (18) 101 kW	CI (18) 102 kW	MNR(18) 70 kW	CI (18) 68 kW
4	CI (18) 58 kW	SHIM (9) 39 kW	CI (18) 123 kW	PTR (10) 113 kW	SHIM (9) 43 kW	LEU (18) 62 kW
5	MNR (18) 35 kW	MNR (18) 62 kW	Refl.	MNR (18) 73 kW	MNR (18) 63 kW	MNR (18) 48 kW
6	LEU (18) 72 kW	SHIM (9) 18 kW	MNR (18) 65 kW	CI (18) 62 kW	REG (9) 36 kW	PTR (10) 49 kW
7	H <sub>2</sub> O	CI (18) 41 kW	PTR (10) 57 kW	PTR (10) 57 kW	MNR (18) 32 kW	Refl.
8	Refl.	Refl.	Refl.	Refl.	Refl.	Refl.
9	H <sub>2</sub> O	H <sub>2</sub> O	H <sub>2</sub> O	Refl.	H <sub>2</sub> O	H <sub>2</sub> O

Legend:

- PTR (10) = 10 plate HEU fuel (8 in all)
- MNR (18) = 18 plate HEU fuel (11 in all)
- CI (18) = 18 plate HEU fuel (9 in all)
- LEU (18) = 18 plate LEU fuel (2 in all)
- SHIM (9) = 9 plate HEU fuel with a control absorber (5 in all)
- REG (9) = 9 plate HEU Regulator Rod (fast-acting shim) (1 in all)
- H<sub>2</sub>O = Water site for irradiation of samples (8 in all)
- Refl. = Reflector / irradiation (10 in all)

# of 18 plate assemblies = 22  
 # of 10 plate assemblies = 8  
 # of control assemblies = 6  
 subtotal = 36  
 # of non-flow sites = 8  
 # of reflector sites (minor flow) = 10  
 Total # of sites = 54

**Figure 3.1** Core Configuration (# 48C) as of January 8, 1997

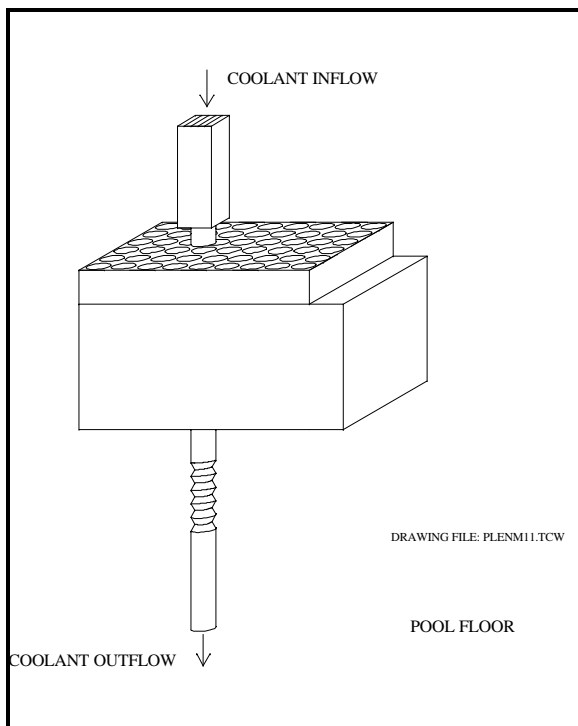


Figure 3.2 Core area of the MNR

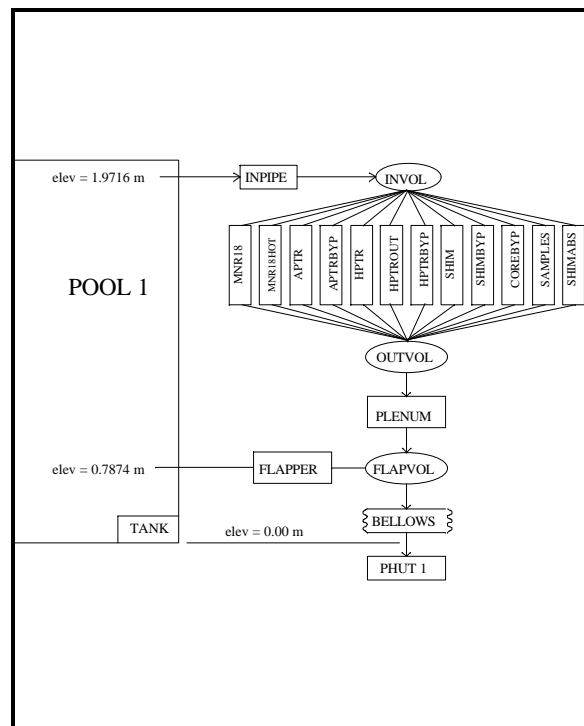


Figure 3.3 Nodal representation of the core

GRID PLATE FUEL ELEMENT HOLE LAYOUT

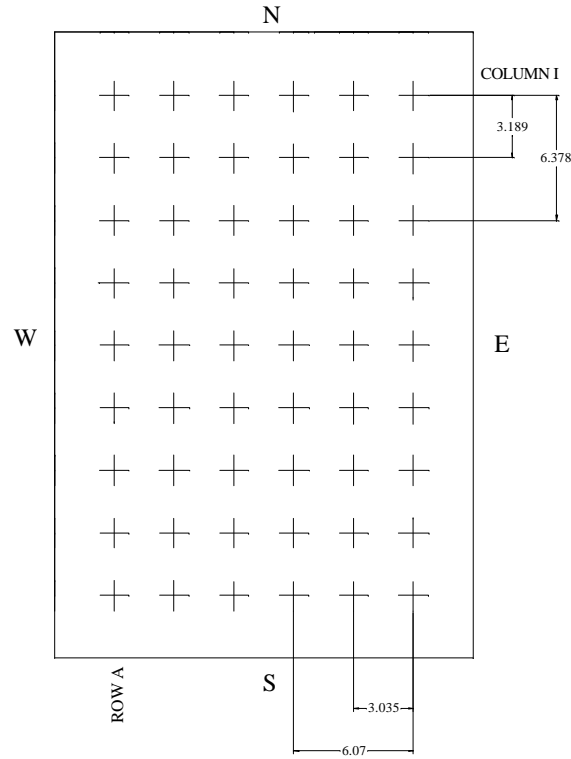


Figure 3.4 Grid plate layout

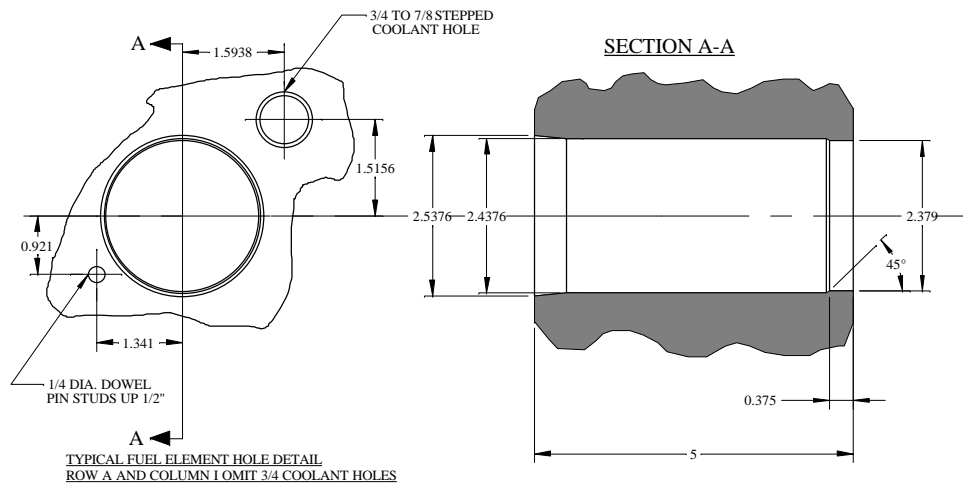


Figure 3.5 Snout hole and bypass hole detail

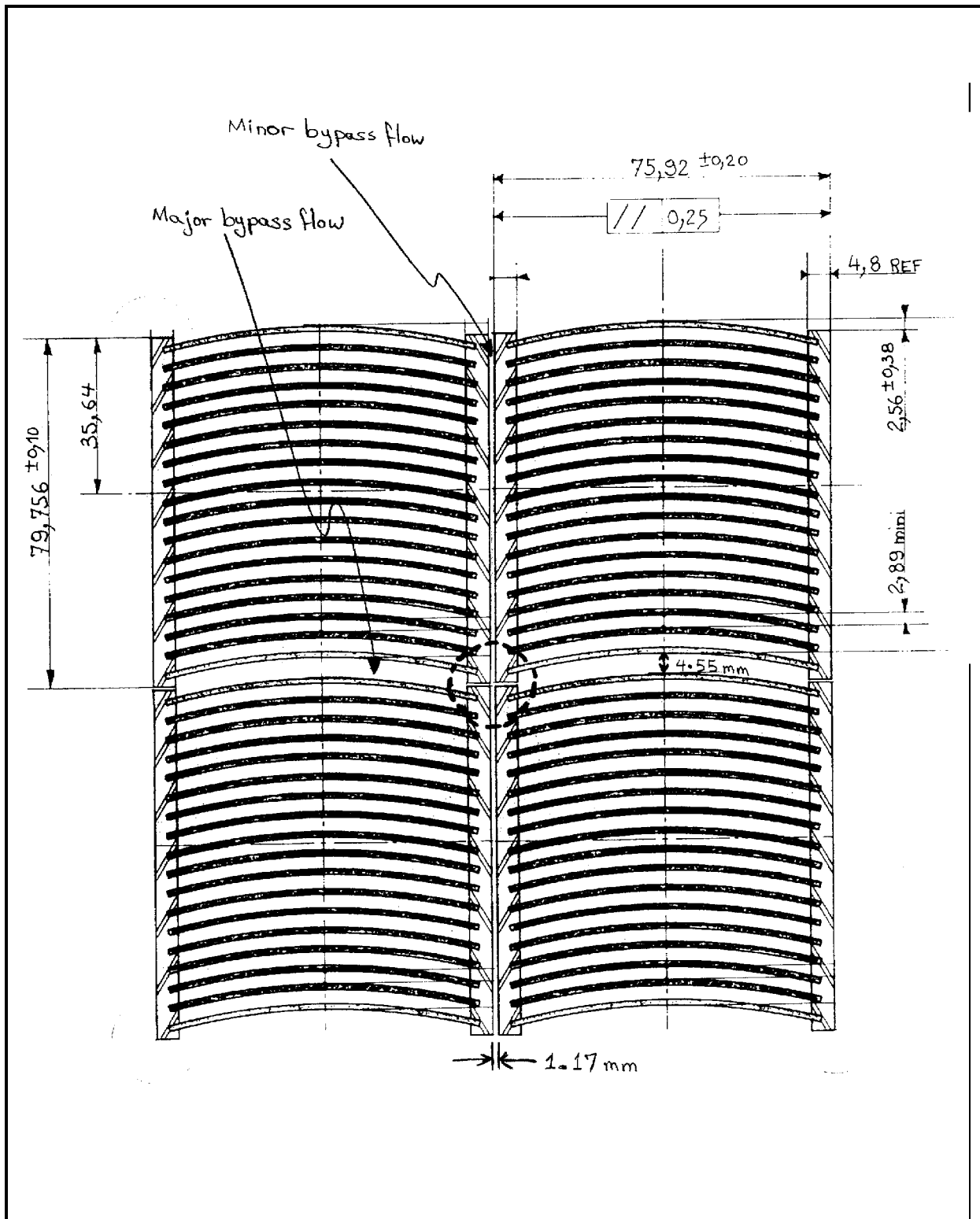


Figure 3.6 Bypass flow geometry in the assembly region

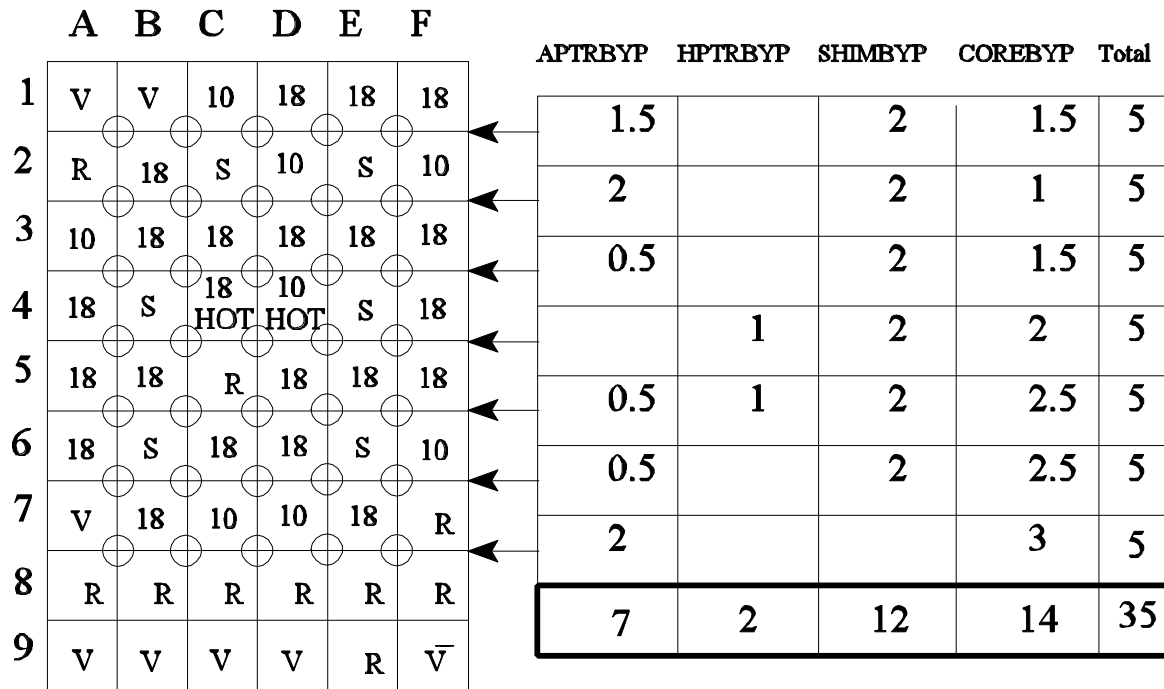


Figure 3.7 Bypass flow assignment

## Chapter 4 System Modelling (CATHENA)

### 4.1 Overview

The Heat Transport System (HTS) schematic flowsheet is shown in figure 4.1. The reactor core is suspended in the pool from a movable support bridge. The core is located near the bottom of the pool. H<sub>2</sub>O coolant flows from the Pool, downward through the core, through the core support grid plate, through a rectangular plenum, through a bellows section and outlet piping into the Holdup Tank (HUT). Both the Pool and the HUT surfaces are at atmospheric pressure. The elevation differences provide the driving force for the HTS flow. Flow is manually controlled by valve V-1.

H<sub>2</sub>O is pumped from the HUT through Heat Exchangers (HXs) and returned to the Pool. Return flow is modulated manually by valve V-13 to match the flow from the Pool to the HUT.

The HTS is represented in the thermalhydraulic computer code CATHENA as a series of nodes and links. The nominal input listing is given in Appendix 1. Figure 4.2 illustrates the nodal representation.

The following describes the input data in some detail. It is assumed that the reader is familiar with CATHENA.

### 4.2 Control Parameters

This section of the input data is for specification of run times, printing, numerics, etc. Nominal or default values are used. In the 'SOLUTION CONTROL' section, the nominal minimum time step ( $10^{-3}$  seconds) is acceptable for modelling thermalhydraulic behaviour. However, for the simulation of rapid neutronics (such as a prompt critical event) the time step was reduced to  $10^{-6}$  seconds.

### 4.3 Components

The COMPONENTS section of CATHENA input specifies the component lengths, areas, hydraulic resistance and elevation changes.

#### 4.3.1 Pool

The Pool is modelled as a TANK component (POOL1) since this will permit the simulation of pool level changes. If AIR was specified in addition to H<sub>2</sub>O as a fluid in the TANK, then all connected components would also need to contain AIR. In addition, a TANK is a closed volume; hence some means of simulating the constant pressure (atmospheric) at the water-air interface is needed. To this end, a RESERVOIR (VENTRES) was connected to the top of the POOL1 via a connecting PIPE (VENTPIPE). The reservoir is assumed to contain saturated steam, not air. The CATHENA representation is shown in figure 4.2.

A limitation of the TANK model is that its cross-sectional area is constant. Hence, variations in pool areas

as a function of level are not represented. This can be augmented by connecting additional tanks at specified elevations as desired should it be deemed necessary. Currently, an average cross-sectional area is used.

The POOL is, in fact, two adjoining pools with a removable gate between them. This gate is normally not used except when maintenance requires pool isolation. Pool volumes are:

Pool	Volume	
	US gallons	m <sup>3</sup>
1	34,500	130.58
2	65,400	247.54
Total	99,900	378.12

#### 4.3.2 Reactor Core

Details of the individual core fuel, control and reflector assemblies are given in chapter 2. The thermalhydraulics of the core as a system of assemblies is given on chapter 3.

#### 4.3.3 PLENUM and BELLOWS

The plenum below the grid plate is a rectangular box as shown in figures 4.3 and 4.4. For the plenum (inside hydraulics):

$$\text{length} = 18'' = 0.5842 \text{ m.}$$

$$\Delta Z = -0.5842 \text{ m.}$$

$$\begin{aligned} \text{cross-sectional area} &= 33'' \times 18.38'' \\ &= 0.8382 \text{ m} \times 0.46685 \text{ m} \\ &= 0.39132 \text{ m}^2 \end{aligned}$$

$$De = \frac{4A}{P} = \frac{4(0.39132)}{2(0.8382 + 0.46685)} = 0.59969 \text{ m.}$$

For the bellows (10" I.D.):

$$\begin{aligned} \text{cross-sectional area} &= \frac{\pi D^2}{4} = \frac{\pi}{4} (0.245)^2 \\ &= 0.05067 \text{ m}^2 \end{aligned}$$

$$\begin{aligned} \text{length} &= 16 \text{ c} + 14 \text{ c} + \text{d} = 31'' \\ &= 0.7874 \text{ m}. \end{aligned}$$

$$\Delta Z = -0.7874 \text{ m}.$$

#### 4.3.4 Flapper

The flapper is a cover for a 15" diameter opening in the side of the plenum. The flapper is normally held closed by the slight pressure difference between the pool and the inside of the plenum caused by the pressure drop through the core (of the order of ½ psi). If coolant flow is reduced below approximately 1100 USGPM, the flapper opens, initiating a reactor trip and permitting thermosyphoning. To model the thermosyphoning flow path in CATHENA, a short PIPE component is added between the POOL and a VOLUME component (FLAPVOL) located the bottom of the PLENUM at elevation 31" (0.7874 m). The flow resistances are uncertain.

#### 4.3.5 Outlet Piping from the POOL to the HUT

The outlet piping from the POOL to the HUT is illustrated in figure 4.5 and the corresponding CATHENA components are shown in figure 4.2.

All the outlet piping is 10" I.D. Thus:

$$\begin{aligned} D_e &= 0.254 \text{ m} \\ \text{Area} &= \frac{\pi D^2}{4} = 0.05067 \text{ m}^2. \end{aligned}$$

One right angle bend has a hydraulic resistance,  $k$ , of approximately 0.32 [CRA57].

The following lists the PIPE COMPONENTS in sequence:

- PHUT1 represents a vertical drop of 1.092 metres from the pool outlet.
- PHUT2 represents a right angle bend and a horizontal run of 2.235 metres.
- PHUT3 represents a right angle bend and a horizontal run of 12.348 metres.
- PHUT4 represents a horizontal run of 1.143 metres. The valve V1 at this location is modelled separately in SYSTEM MODELS section of CATHENA input.
- PHUT5 represents a 96° bend and a horizontal run of 3.835 metres.
- PHUT6 represents a 120° bend and a horizontal run of 2.249 metres.
- PHUT7 represents a 135° bend, a horizontal run of 3.200 metres, a Tee and gate valve V10.
- PHUT8 represents a vertical rise of 1.600 metres to the HUT.

#### 4.3.6 Holdup Tank (HUT)

The HUT is modelled via a TANK component as per the POOL. The air surface is modelled as by a RESERVOIR component (VHUT) connected to the HUT via an arbitrary PIPE COMPONENT, VHUTPIPE,

as depicted in figure 4.2.

#### 4.3.7 Inlet Piping (HUT to Pump Suction)

The inlet piping (HUT to Pump Suction) CATHENA components are shown in figure 4.2. All the inlet piping is 10" I.D as per the piping from the Pool to the HUT unless otherwise specified.

The following lists the PIPE COMPONENTS in sequence:

- HUTPMP1 represents an inclined drop of 0.381 metres, with a pipe length of 1.245 metres, from the HUT outlet.
- HUTPMP2 represents a right angle bend and a horizontal run of 1.092 metres.
- HUTPMP3 represents a horizontal run of 0.461 metres. The valve V12 at this location is modelled separately in the SYSTEM MODELS section of CATHENA input.
- HUTPMP4 represents a horizontal run of 1.000 metres and two Tees.
- HUTPMP1 represents a VOLUME for the pump bypass connection.
- HUTPMP4a represents a horizontal run of 0.727 metres and three Tees.

#### 4.3.8 Inlet Piping (Pump to Heat Exchangers)

The inlet piping (Pump to Heat Exchangers) CATHENA components are shown in figure 4.2. All the inlet piping is 10" I.D as per the piping from the Pool to the HUT unless otherwise specified.

The following lists the PIPE COMPONENTS in sequence:

- PMPHX1 represents a horizontal run of 1.521 metres. The associated HT pump and check valve are modelled separately in the SYSTEM MODELS section of CATHENA input.
- PMPHX2 represents a horizontal run of 7.490 metres and one Tee.
- PMPHX3 represents a right angle bend and a horizontal run of 0.762 metres.
- PMPHX4 represents a right angle bend and a vertical rise of 1.803 metres to the heat exchanger inlet flange.

#### 4.3.9 Inlet Piping (Heat Exchangers to Pool)

The inlet piping (Heat Exchangers to Pool) CATHENA components are shown in figure 4.2. All the inlet piping is 10" I.D as per the piping from the Pool to the HUT unless otherwise specified.

The following lists the PIPE COMPONENTS in sequence:

- HX1IN represents the inlet nozzle to Heat Exchanger 1 (HX1), a vertical run of 0.1 metres (not verified).
- HX1 represents the internal flow path (shell side) through HX1. No attempt was made to model this accurately.
- HXFLG represents the outlet nozzle of HX1 and the inlet nozzle of HX2 by a vertical run of 0.1 metres (not verified).
- HX2 represents the internal flow path (shell side) through HX1. No attempt was made to model this accurately.
- HX2OUT represents the outlet nozzle to HX2, a vertical run of 0.1 metres (not verified).
- HXP1 represents a vertical run of 1.118 metres and gate valve V-15.
- HXP1 represents a VOLUME for the pump bypass connection.

- PMPBYP represents the pump bypass line, a 6" ID (15.24 cm) pipe running from a Tee downstream of the Heat Exchangers through valve V-13 to a Tee upstream of the HT pump. The cross sectional area is 182.4 cm<sup>2</sup>. The elevation drop is 5.258 metres. A run length of 6 metres is used (not verified). Valve V-13 is modelled separately in the SYSTEM MODELS section of CATHENA input and is controlled by the HUT level controller, HUTLVL, modelled in the SYSTEM CONTROL section of CATHENA input.
- HXP2 represents a right angle bend and a horizontal run of 6.299 metres.
- HXP3 represents a right angle bend and a horizontal run of 4.302 metres.
- HXP4 represents a right angle bend and a vertical drop of 1.245 metres.
- HXP5 represents a right angle bend and a horizontal run of 3.381 metres.
- HXP6 represents a right angle bend and a vertical drop of 4.470 metres.
- HXP7 represents a right angle bend and a horizontal run of 2.245 metres.
- HXP8 represents a 150° angle bend, a Tee and a horizontal run of 0.965 metres.
- HXP9 represents butterfly valve V-2 and a horizontal run of 9.373 metres.
- HXP10 represents a right angle bend and a horizontal run of 2.210 metres.
- HXP11 represents a right angle bend and a vertical rise of 0.838 metres to the pool inlet.

#### 4.4 Connections

The CONNECTIONS section of CATHENA input links the components together. Specification is straightforward. Of note are the levels for the connections of the TANK components. The top of the core is at elevation 1.982 m (6' 6"). The connection to the tank is made at 1.9812 m to 2.0 m, i.e. at 2.0 m, air ingress is assumed to start should the pool level drop this low.

The reservoirs are connected near the top of the POOL and HUT.

#### 4.5 Boundary Conditions

The reservoirs are nominally at 101 kPa, representing atmospheric pressure. Recall that the air is modelled as saturated steam since the inclusion of an additional component (air) is an unnecessary complication.

#### 4.6 System Models

##### 4.6.1 HT Pump

The HT pump model is not a critical component since the return flow to the pool only affects the core flow indirectly, that is, via pool level. Hence, the ANC pump model was selected. The rated flow is 120 kg/s at a  $\Delta P$  of 296 kPa at 1750 rpm. Thus:

$$\begin{aligned} \text{head}(m) &= \frac{\Delta P}{\rho g} = \frac{296 \times 1000 \text{ Pa} (= \text{kg}/m\text{-sec}^2)}{995 \text{ kg}/m^3 \times 9.81 \text{ m}/\text{sec}^2} \\ &= 30.32 \text{ m}. \end{aligned}$$

volumetric flow (m<sup>3</sup>/sec)  $\approx$  0.120 m<sup>3</sup>/s.

The k of the pump when stopped was set at 100 (arbitrarily). Reverse flow through the pump will be zero in any case since there is a check valve at the pump discharge, preventing backflow.

#### 4.6.2 HT Heat Exchangers

There are two primary to secondary side shell and tube heat exchangers. They are connected in series.

Like the HT pumps (and all other HUT  $\rightarrow$  Pool return flow components), exact modelling is not critical.

Nominal values for areas, heat transfer coefficients, etc. are currently used. The average primary side (shell side) HX inlet temperature is about 32°C. The nominal secondary side (tube side) temperature is 20°C but this is subject to seasonal variation. To satisfy  $Q = UA \Delta T$ ,

$$UA = \frac{1 \times 10^6 \text{ watts}}{12^\circ\text{C}} = 83300 \text{ watts}/^\circ\text{C}.$$

For a guessed area of 100 m<sup>2</sup>, the U required is 833 watts/m<sup>2</sup>°C, assuming a linear temperature profile.

#### 4.6.3 HTS flow control (V-1 and V-13)

The MNR has manual flow control only. Normally, valve V-1 at the pool outlet is throttled to limit the core flow. Then valve V-13 is opened to provide pump recirculation and thus flow control on the return leg. The two flows (outlet from the pool and return to the pool) are thus equalized.

For simulation purposes, V-1 is manually adjusted to yield the desired core flow and V-13 is controlled to maintain HUT level. System models are required in CATHENA for modelling valve motion.

The pump bypass line is 6" I.D. Valve V-13 is a gate valve. Valve V-1 is a butterfly valve. Standard CATHENA ASME models are used.

#### 4.6.4 Flapper control

To simulate the flapper position, a manual valve model is used. The nominal valve position is 0.0 (closed). The valve position can be set to 1.0 (open) for the thermosyphoning case.

#### 4.6.5 HT pump check valve

The standard ASME check valve model is used to simulate the check valve at the HT pump outlet.

#### 4.6.6 Core entrance and exit hydraulic losses

Junction resistances are manually applied to the core inlet and outlet using the JUNCTION RESISTANCE

model. The large area changes at the inlet and outlet of the flow passages between the fuel plates implies a  $k$  of 0.5 at the inlet and 1.0 (complete kinetic head loss) at the outlet.

#### 4.6.7 Shim absorber and sample holder orifices

The small holes that restrict the flow through the central coolant passages in the shim absorber and sample holder assemblies are modelled by the standard ASME orifice models.

#### 4.6.8 Reactor Kinetics

CATHENA reactor physics is limited to point kinetics. The  $\beta$ 's and  $\lambda$ 's for the delayed neutrons are values for U-235 since the core is composed of highly enriched uranium and plutonium buildup is small.

Optionally, a specified power history can be supplied but the kinetics model was implemented for the simulation of loss of regulator (LOR) accidents.

Xe is neglected since only short term transients are of interest.

MNR has an inherent negative reactivity coefficient for the fuel temperature, the water temperature and the water density. The measured temperature coefficient at MNR is 0.0684 mk / °C above 34 °C . Reactor physics analysis has not proceeded sufficiently at the moment to yield the required reactivity coefficients and measured coefficients for the individual effects of fuel temperature and water temperature are not available. A measured void coefficient is also not available. In the interim, an IAEA benchmark study for a similar core [TR97-05] is used. The CATHENA 'DIF' input option, wherein reactivity coefficients are with respect to the steady state at time = 0, is used. From the IAEA study:

Water temperature coefficient:

$$\Delta\text{reactivity} = -0.1188 \text{ mk}/^\circ\text{C} * \Delta T$$

Fuel temperature coefficient:

$$\Delta\text{reactivity} = -0.0006 \text{ mk}/^\circ\text{C} * \Delta T$$

Density temperature coefficient:

$$\Delta\text{reactivity} = 0.260 \text{ mk}/(\text{kg}/\text{m}^3) * \Delta\text{density} - 0.000335 \text{ mk}/(\text{kg}/\text{m}^3)^2 * (\Delta\text{density})^2$$

Further work is in progress on the temperature and void reactivity feedback coefficients.

## 4.7 System Control

### 4.7.1 Flow Control

As discussed in the previous system, the HUT level is maintained at the desired setpoint by controlling the pump bypass flow. A standard PI controller is used. The gain and time constant used do not relate to reality since there is no actual controller in MNR. This controller is for simulation convenience only.

### 4.7.2 Regulation Rod Control

A PD controller is used to simulate the reactor regulation system (RRS). The model is an interim one only for testing purposes. This will be updated in due course to reflect the actual control but fidelity is not required since most accident scenarios involve either constant power or a failed RRS. There are a few scenarios involving small reactivity insertions due to irradiation sample mishandling. But these accidents are benign.

#### 4.7.3 Shim Rod Worth

The bank of 5 shim safety rods that are inserted by gravity upon a reactor trip have a total worth of approximately 92 mk. The insertion delay time has been tested to be 25 ms and the rod drop time is approximately 0.5 s.

#### 4.7.4 Reactor Trips

The following reactor trips are simulated:

- high power (125%)
- high log rate (reactor period less than 4 seconds)
- low primary flow (LFP) (1500 USGPM)

To be added are:

- flapper open trip (FO)
- low pool level (LPL)

The reactor period trip is not fully implemented at the time of writing of this report.

## 4.8 Initial Conditions

The initial conditions supplied to CATHENA are those appropriate to steady state operation at 2 MW. Since CATHENA does not have a steady state simulation option, it is necessary to run the code to steady state before event scenario transients are simulated.

Initial Pool and HUT levels are supplied in this section. The nominal pool level is 30' 5" (9.271 m). The HUT level varies over time mainly due to pool water evaporation. Makeup water is added in batches from time to time to keep the HUT level between 2 and 3 metres.

## 4.9 Heat Transfer Package

Currently six heat transfer models have been developed:

- MNRFUEL: average 18 plate assembly
- MNRHOT: highest power 18 plate assembly
- PTRFUEL: average 10 plate assembly
- PTRHOT: highest power 10 plate assembly

- SHIMFUEL: average shim assembly
- HMAPLE: highest power MAPLE assembly.

The details of the hydraulic and heat transfer models for the core have been discussed in Chapters 2 and 3.

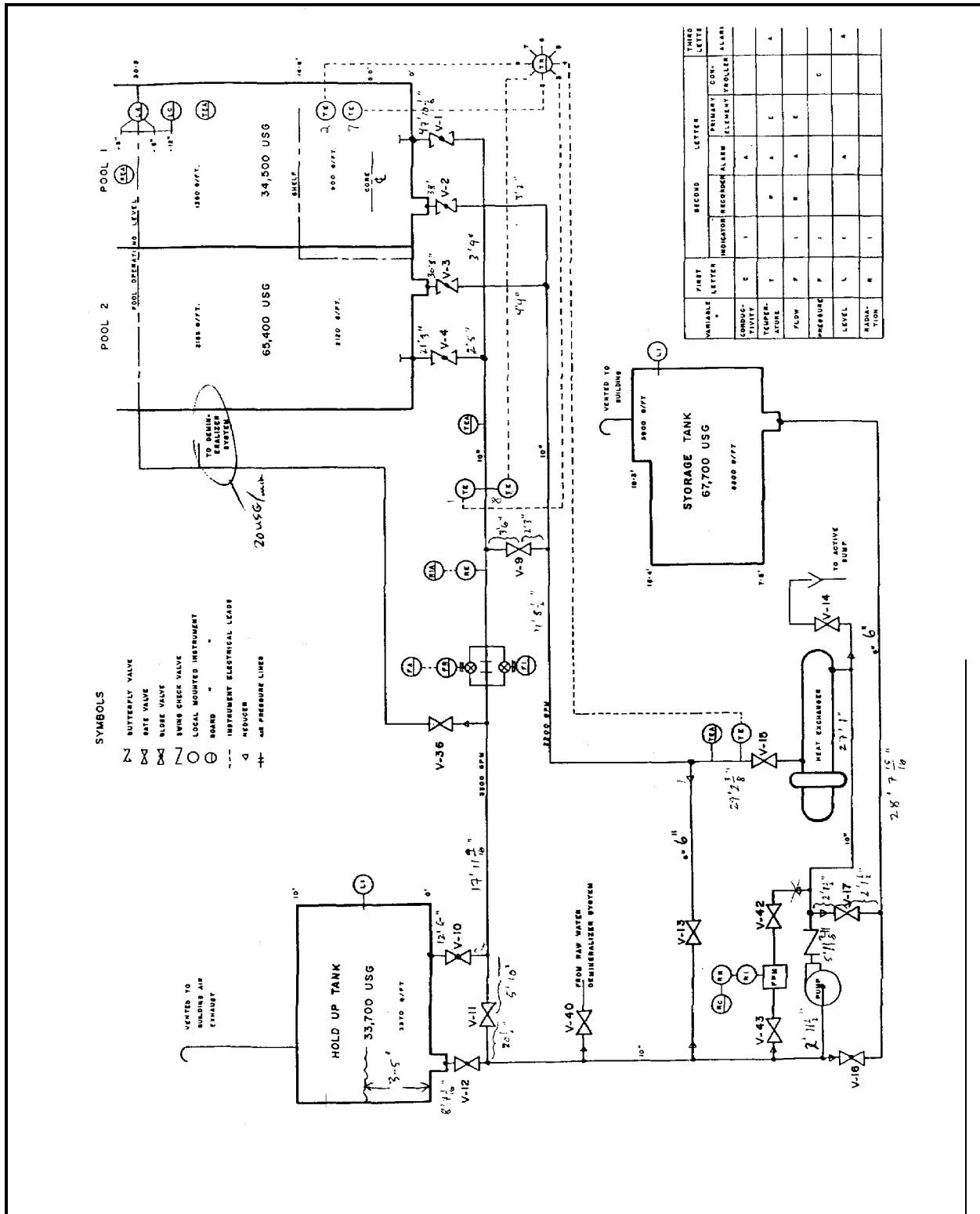


Figure 4.1 McMaster Nuclear Reactor flowsheet

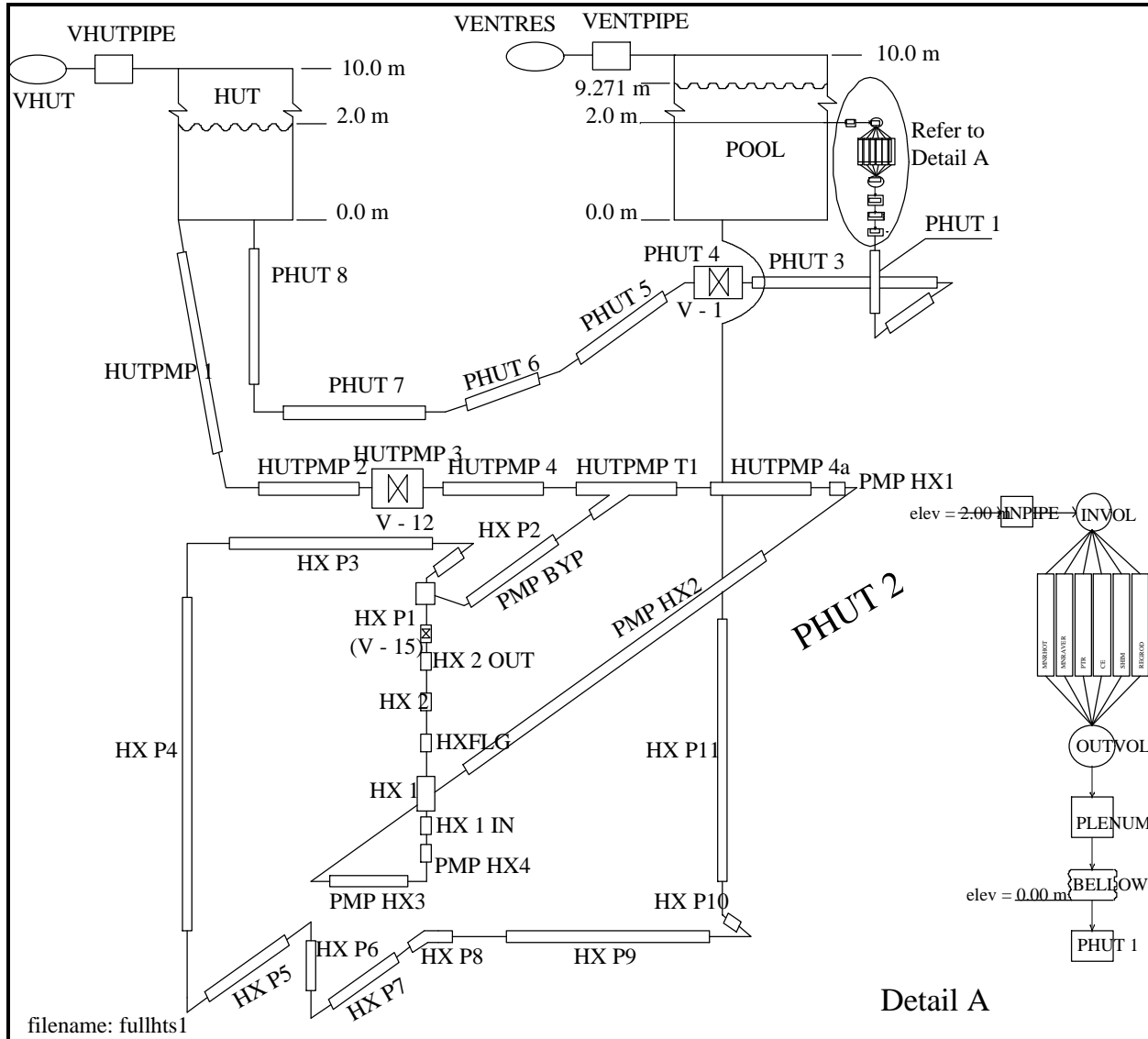


Figure 4.2 CATHENA representation of MNR

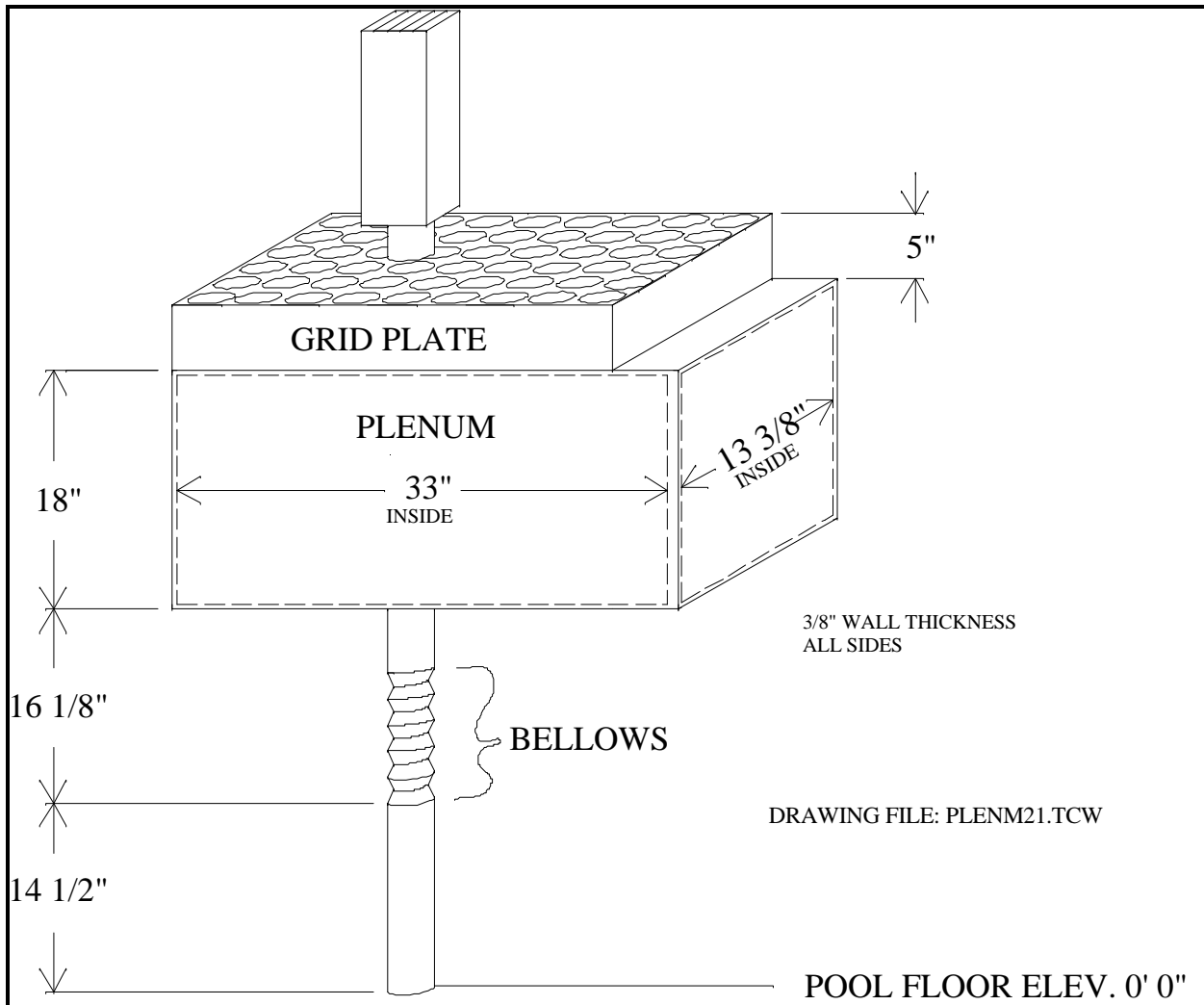
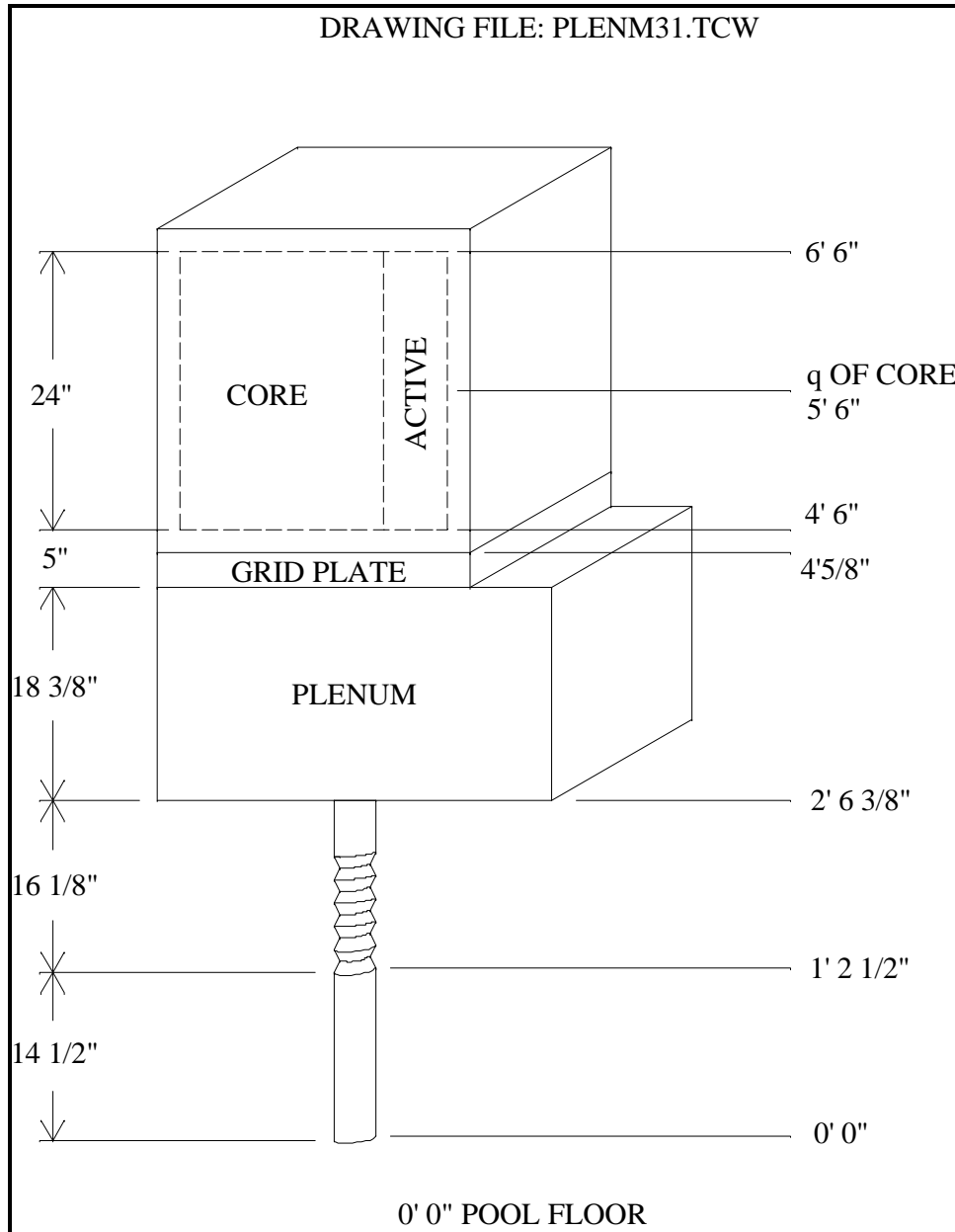


Figure 4.3 Plenum region



**Figure 4.4** Elevations in the core area

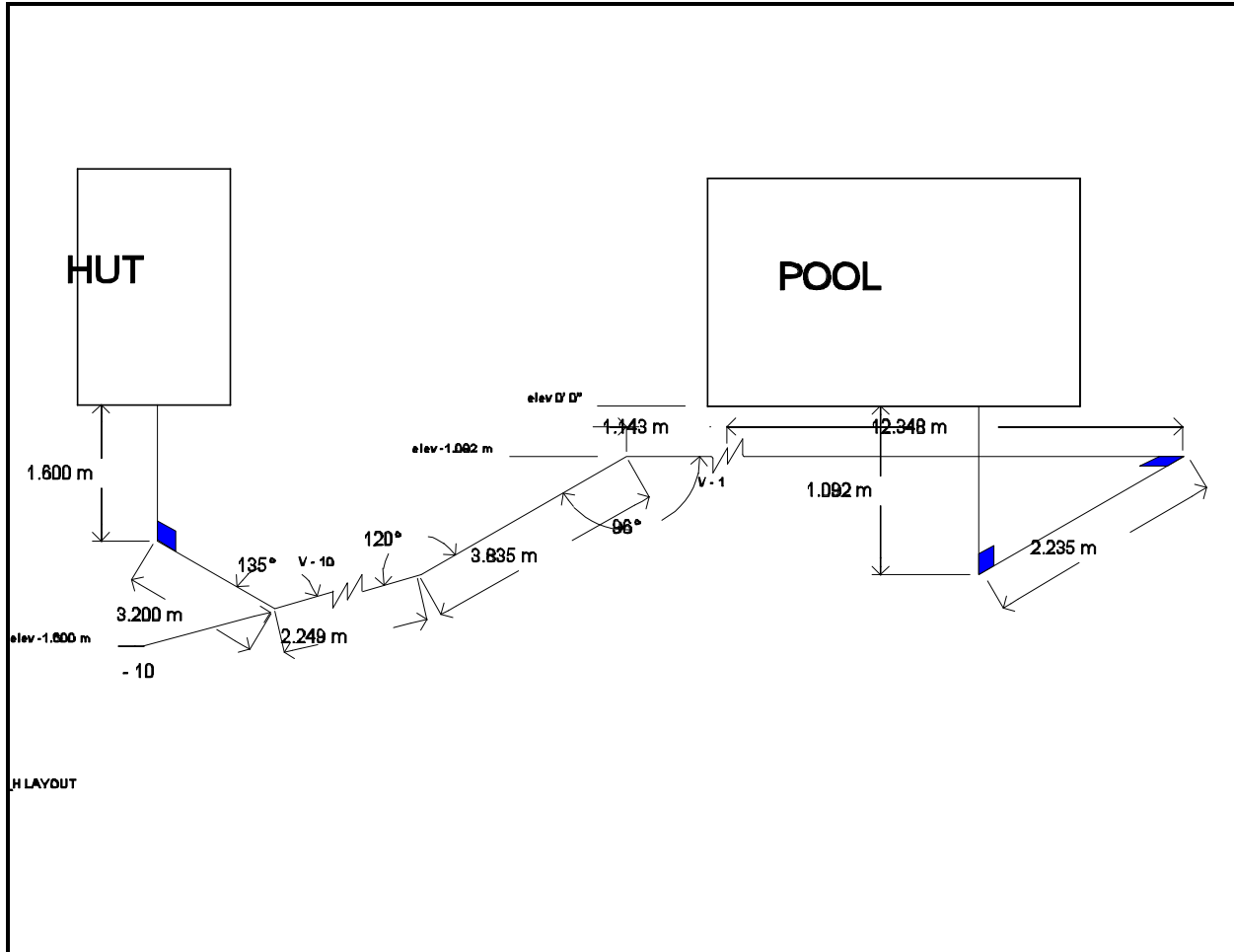


Figure 4.5 Outlet piping layout

## Chapter 5 CATHENA Test and Scoping Runs

The following discusses, in chronological order, the testing of the CATHENA model for MNR as it was systematically developed.

### 5.1 Edward's Pipe Blowdown

The initial task was to become familiar with CATHENA. To this end, the standard Edward's pipe blowdown case was simulated as per an example input file supplied by AECL. AECL staff monitored the process and verified that the user was correctly running CATHENA and that the input and output of the test case was as expected.

Archive directory: /cathena/development/asample1.

### 5.2 MAPLE Pin Test Loop

AECL supplied a test problem description for an electrically heated MAPLE pin simulation test loop. The boundary conditions were fixed inlet pressure and flow. The test case was prepared and run. AECL staff reviewed the input and output and verified that the results were as expected.

Archive directory: /cathena/development/asample2.

### 5.3 MAPLE Single Pin for MNR Conditions

The previous test case was modified to reflect the flow and power conditions of the MNR reactor.

The flow area per pin =  $37.128 \text{ cm}^2 / 24 = 1.547 \times 10^{-4} \text{ m}^2$

The mass flow rate is

$$\begin{aligned} W &= \rho VA = 995 \frac{\text{kg}}{\text{m}^3} \times 1 \frac{\text{m}}{\text{s}} \times 1.547 \times 10^{-4} \text{ m}^2 \\ &= 0.15393 \text{ kg/s} \end{aligned}$$

The power chosen was

$$\frac{2000 \text{ kW}}{35 \text{ assemblies} \times 24 \text{ pins/assembly}} = 2.38 \text{ kW/pin}$$

An extreme peak/average power of

$$\left(\frac{\pi}{2}\right)^2 = 2.467$$

was chosen to give a pin power of 5.87 kW (rounded up to 6 kW). The results show a peak heat flux of 567 KW/m<sup>2</sup> and a CHF of 6064 kW/m<sup>2</sup>. A more reasonable peak to average power of 1.5 yields a pin power of 2.38×1.5 = 3.57 kW. Thus the corrected CPR is

$$CPR_{2MW} = \frac{6064}{567} \times \frac{6}{3.57} = 18.0$$

This is based on the MAPLE correlations in CATHENA and an assumed nominal velocity of 1 m/s. Subsequent simulations include a system model so that flow variations can be factored in.

Archive directory: /cathena/development/mnr-maple.

## 5.4 Single Plate Assembly

By way of comparison an 18 plate assembly was simulated for similar conditions to that of Section 5.3. A peak to average power of 2.38 was chosen (incorrectly) to give a peak assembly power of 136 kW (compared to 57.14 kW for the average assembly). For this case, CATHENA did not calculate the CHF because the heat flux was too low to bother!

Raising the power to 5×136 kW = 680 kW/assembly gave a CPR of 4.66. Correcting this CPR gives

$$CPR_{2MW} = 4.66 \times \frac{680}{57.14 \times 1.5} = 37.0$$

As expected, this is roughly twice the MAPLE case. Subsequent simulations include a system model so that flow variations can be factored in.

Archive directory: /cathena/development/mnr-plate.

## 5.5 MNR Plate Core Simulation (all 18 plate assemblies)

To investigate the flow distribution that might result when assemblies are at various powers, subject to the same inlet and outlet boundary conditions, the CASE #4 model was modified to include 34 average assemblies and one peak power assembly in parallel. The peak / average power used was 1.5. The inlet pressure and flow from the upstream reservoir provided the boundary conditions and permits a core flow redistribution based on local assembly conditions. The heat transport system from pool to HUT is not simulated.

The nominal run at 2 MW core power did not invoke the CHF calculation. At ~ 20 MW however

$$CPR = \frac{3,372,792 \text{ W}}{920521 \text{ W}} = 3.2096$$

The corrected  $CPR_{2MW} = 32$ .

This drop from the single assembly case ( $CPR=37$ ) results from a reduction in the flow of the high power channel (1.0 m/s  $\rightarrow$  0.85 m/s).

Archive directory: /cathena/development/mnr-core.

## 5.6 HT System Flow Lock-On

To lock the CATHENA simulation onto the actual plant performance, the current 2 MW operation was simulated, complete with HTS piping.

The HUT level varies during operation over the weeks due to pool water evaporation. A nominal level of 3.0 metres was chosen for the simulation tests. Valve V-1 was throttled until the steady state core flow was 1600 USGPM (100.94 l/s), which is equivalent to a fuel assembly velocity of 0.836 m/s. The required valve position was 0.33 open for a velocity of 0.85 m/s.

On Dec. 10, 1996, the operating conditions were:

Core flow: 1590 USGPM

Valve V-1 position: 0.25 open

HUT level: 5' 8" (1.72 m)

If the simulation used a HUT level of 1.72 m, then V-1 would need to be closed still further, moving it closer to the measured valve. However, further refinement is meaningless since the indicated valve position is only approximate and since the hydraulic resistance of a butterfly valve is a highly non-linear function of valve position.

The important item to note is that the bulk of the hydraulic resistance is in the outlet piping, not the fuel assemblies, hence changes in core conditions will have little effect on overall system flow. This includes changes due to bulk fuel design changes or due to bulk core voiding. Redistribution of core flows can, of course, occur due to local effects such as differential fuel design changes or differential voiding.

Further, the bulk of the outlet piping resistance is in valve V-1 at the current conditions. This will not necessarily be the case at 5 MW operation.

Archive directory: /cathena/development/mnr-sys.

## 5.7 HT System $\Delta T$ Lock-On

The typical core  $\Delta T$  at 2 MW operation is measured at 4.8°C. The simulation gives 5°C (only one significant figure is used in the standard output).

The overall heat transfer coefficient in the HXs was increased to  $875 \text{ W/m}^2\text{°C}$  (from  $833 \text{ W/m}^2\text{°C}$ ) to provide a pool inlet temperature of  $34\text{°C}$  to match the measured pool temperature. The actual temperatures vary seasonally.

Archive directory: /cathena/development/mnr-sys.

## 5.8 Low Power Thermosyphoning

In preparation for the simulation of the January 1994 power excursion, the system was simulated at low power with the HTS pump turned off, the pool and HUT isolated and the flapper open. This exercise revealed that the flapper model required minor modification and that the heat transfer coefficients at the vapour - liquid interface in the TANK models for the pool and HUT should be set to 0. The revised model gave the expected qualitative behaviour of upflow through the core at low power with the flapper open.

The thermosyphoning flow is sensitive to the hydraulic resistances in the core area. No direct flow measurements under thermosyphoning conditions are available for MNR. It is possible to infer a flow from core  $\Delta T$  measurements, although the inference will be imprecise. It is hoped that such an experiment will take place in the near future.

Archive directory: /cathena/development/mnr-pk.

## 5.9 MNR Current Plate Core Simulation

To reflect a realistic core configuration, the initial core model of 34 average 18 plate assemblies and 1 high power assembly was modified to include 21 average power and 1 high power 18 plate assemblies, 7 average power and 1 high power 10 plate assemblies, and 6 shim assemblies. The assembly powers were as measured on January 8, 1997, as given in chapter 3. The simulation results show, as expected, that the larger flow areas of the 10 plate assemblies give a lower resistance flow path. This results in a larger assembly flow in the 10 plate fuel than in the 18 plate fuel. However, the higher power per plate in the 10 plate fuel gives rise to slightly higher centreline fuel temperatures in the 10 plate fuel than in the 18 plate fuel. The results are summarized in table 5.1.

The core velocity is limited by the pool-HUT elevation differences and the HTS piping resistances, NOT the core resistance. The gross flow is measured so we are only concerned about flow distribution between the assemblies. The bulk of the assembly resistance is due to the inlet and outlet losses (total  $k \sim 1.5$ ). Since the 10 plate and 18 plate assemblies are geometrically similar, the CATHENA model should be a fair representation. In situ flow measurements of replica fuel assemblies [RUM88] show the flow in the 18 plate assembly to be 70% of the 10 plate. That agrees with the CATHENA prediction as shown in table 5.1.

**Table 5.1** Flows and temperatures for MNR (base case: core 48c)

ASSEMBLY GROUP	COOLANT VELOCITY (m/s)	FLOW / ASSEMBLY (kg/s)	COOLANT OUTLET TEMP (°C)	MAXIMUM SHEATH SURFACE TEMP (°C)	MAXIMUM FUEL TEMP (°C)
MNR18	0.72	49.20	36	43	44
MNR18HOT	0.73	2.35	43	59	60
APTR	1.00	27.28	34	45	46
APTRBYP	0.72	2.21	36	47	48
HPTR	1.00	3.03	37	59	62
HPTROUT	1.00	0.87	34	59	62
HPTRBYP	0.72	0.63	34	63	65
SHIM	0.72	7.43	34	45	46
SHIMBYP	0.73	3.80	36	46	47
COREBYP	0.72	4.43			
SAMPLES	0.03	0.03			
SHIMABS	0.06	0.03			

Archive directory: /cathena/development/mnr-grid.

---

## **Chapter 6      Conclusion**

### **6.1    MNR Plate Assembly Margin**

Based on initial CATHENA runs, the current operating margin before the onset of a heat transfer crisis is considerable since the CPR is in the range of 10 - 30.

### **6.2    MNR-MAPLE Pin Assembly Margin**

Initial estimates indicate that the MAPLE pin design is roughly a factor of 2 less in heat transfer area compared to the plate design. However, given that a heat transfer crisis for a low velocity, low pressure reactor like MNR is more dependent on the onset of significant void rather than heat flux per se, the MAPLE configuration may approach the plate fuel design in CPR margin.

### **6.3    Code Lock-On**

The CATHENA code appears to model the actual plant performance adequately. Comparison is on-going.

## References

- CAT95 -, "CATHENA MOD-3.5 / Rev 0, Theoretical Manual", Atomic Energy of Canada Limited, ed. B.N. Hanna, RC-982-3, 1995.
- CRA57 -, "Flow of fluids through Valves, Fittings and pipes", Crane Canada Ltd., Technical Paper No. 410-C, 1957.
- ERN72 P.C. Ernst, "MNR Heat Transfer Calculations", McMaster Nuclear Reactor Technical Report, 1972.
- HAA84 L. Haar, J. Gallagher and G Kell, 1984 NBS/NRC Steam Tables, McGraw-Hill International, Toronto.
- INC90 Frank P. Incropera and Davis P. DeWitt, Introduction to Heat Transfer, John Wiley & Sons, Second Edition, ISBN 0-471-61247-2.
- MIC77 -, "Utilization of Intermetallic Uranium Aluminide (UAl<sub>3</sub>, UAl<sub>4</sub>, UAl<sub>2</sub>) and Uranium Oxide (U<sub>3</sub>O<sub>8</sub>, UO<sub>2</sub>) Cermet Fuel Cores in the Ford Nuclear Reactor", Safety Analysis Report for the Ford Nuclear Reactor, University of Michigan, prepared for the U.S. Nuclear Regulatory Commission, License R-28 Docket 50-2, June 1977.
- MIR59 S. Mirshak, W.S. Durant, and R.H. Towell, "Heat Flux at Burnout," AEC R&D Report DP-355, E.I. du Pont de Nemours & Co., Aiken, South Carolina, 1959 February.
- MIS87 K. Mishima and H. Nishihara, "Effect of Channel Geometry on Critical Heat Flux for Low Pressure Water," Int. J. of Heat & Mass Transfer, Vol. 30, No. 6, 1169-1182 (1987 June)
- OBE69 C.F. Obenchain, "PARET -- A Program for the Analysis of Reactor Transients", AEC Research and Development report IDO-17282, U.S. Atomic Energy Commission, January 1969.
- RUM88 Helena E.C. Rummens, "Thermalhydraulic Studies of the McMaster Nuclear Reactor Core", M.Eng Thesis, Department of Engineering Physics, McMaster University, April 1988.
- TR97-05 Hassan Basha, "Reactor Physics Analysis of the McMaster Nuclear Reactor, McMaster Nuclear Reactor, MNR Technical Report 97-05, April 28, 1997.

---

## **Appendix 1    Typical CATHENA Input File Listing**

(Not reproduced in this on-line version of the report)